Oxygen reduction reaction electrocatalysis in neutral media for bio-electrochemical systems

Carlo Santoro[1], Paolo Bollella[2], Benjamin Erable[3], Plamen Atanassov[4], Deepak Pant[5]*

[1] Department of Material Science, University of Milano-Bicocca, Building U5, Via Cozzi 55, 20125 Milan, Italy
[2] Department of Chemistry, Università degli Studi di Bari A. Moro, Via E. Orabona 4, 70125 Bari, Italy
[3] Laboratoire de Génie Chimique, Université de Toulouse, CNRS, INPT, UPS, Toulouse, France
[4] Department of Chemical & Biomolecular Engineering and National Fuel Cell Research Center, University of California Irvine, Irvine, CA 92697, USA
[5] Separation and Conversion Technology, Flemish Institute for Technological Research (VITO), Boeretang 200, Mol 2400, Belgium

Email: deepak.pant@vito.be

Abstract

Oxygen reduction reaction (ORR) is an electrochemical process with uppermost importance to energy conversion and storage, corrosion and chemical technologies. It plays a major role in biological processes (respiratory biochemical chain of reactions) and is being incorporated in numerous bio-electrochemical devices and systems: microbial and enzymatic fuel cells, micro-biosynthesis processes, water desalination and purification technologies and biosensing. Researchers from various backgrounds are joining to address the specifics of ORR in close-to-neutral environments, in the light of their possible integration with bioprocesses. Understanding the ORR mechanism in this pH region is complex as it involves biotic (living systems or components derived thereof) and abiotic (often inorganic materials or composite) catalysts. This review offers a summary of catalyst class-dependent ORR mechanisms and pathways with corresponding limiting steps relevant to the practical use in bio-electrocatalytic systems. We analyse the technological challenges often caused by the use of oxygen depolarisation as main driving force in practical applications.

Introduction

Oxygen in its gaseous form or dissolved (DO) in the electrolyte is probably the most frequently used reagent/oxidant in electrochemical systems due to its specific features[1]. The oxygen reduction reaction (ORR) is one of the most studied reaction in electrochemistry and often the limiting reaction of the overall electrochemical system[1,2]. Oxygen electrochemistry enables many technical advances in energy technology (fuel cells

and water electrolysis), energy harvesting from ubiquitous sources, waste transformation and water purification, desalination, soil remediation, etc. Integrating biocatalysts (microorganisms and biofilm, enzymes and cellular extracts) into electrochemical technology requires a pH match between the ORR — most effective at extremely high and low pH — and the operational stability of the biotic component. The sluggish ORR kinetics is strongly pH dependant, and is restrained in close to neutral (circum-neutral) media. Under circum-neutral pH operating conditions, the concentration of both protons (more precisely hydronium cations) and hydroxide anions are several orders of magnitude lower compared to extreme pHs[3]. As a result, in circum-neutral media the performance of bioelectrochemical systems (BESs) is dramatically lower compared to chemical fuel cells. However, understanding those limitations and addressing them is important for several practical applications such as power generation from ubiquitously available fuels, hydrogen production, water desalination, production of value-added products in processes conjugated with carbon capture and biosensing. Inorganic electrocatalysts have been inherited from chemical fuel cells and widely used in BESs, sometimes being the most effective electrocatalysts during operations. In parallel, due to their natural compatibility with neutral electrolyte environments, biocatalysts such as enzymes, multi-enzyme macro-complexes or whole microorganisms have been explored as effective ORR electrocatalysts[4-6]. However, the addition of biological matter, acting as bio-electrocatalyst significantly increases the level of complexity of an already complex ORR process occurring over inorganic electrocatalysts.

This review focuses initially on the description of the ORR mechanism highlighting each reaction step and the critical/rate-limiting steps. The analysis of the ORR occurring over inorganic electrocatalysts highlighting electron transfer (ET) mechanisms and limitations is reported. The description of the enzyme-catalysed ORR focusing on the ET mechanism, limitations and applications in enzymatic electrochemical systems (EESs) is also presented. Moreover, the ORR mechanism occurring in the bacterial electrocatalysts, the corresponding ET mechanisms, rate-limiting steps involved in the process, bacterial formation and growth and its activity in microbial electrochemical systems (MESs) are reported. Different cathode architectures are identified and reported indicating their relative advantages and disadvantages. Moreover, the scaling up of the cathodes used in BESs is presented. Finally, the perspective and future directions related to the ORR operating in close to neutral pH ($6<pH<9$) are discussed.

Overview of ORR mechanism

The use of abiotic (inorganic or composite) electrocatalysts in BES is the most immediate, as those have been most studied and developed within the mainstream electrochemical low temperature acidic and alkaline fuel cell technology. In the case of inorganic electrocatalysts, ORR can follow different ET mechanisms that can be summarised into a $4e^-$, $2e^-$ or $2+2e^-$ transfer mechanism[7]. A direct $4e^-$ transfer mechanism is preferred and is the most efficient in transforming reagents to final products. A partial

reduction of oxygen following a $2e^-$ transfer mechanism can also occur, but it is less efficient, and the reaction is better known as hydrogen peroxide generation reaction (HPGR). A more complex $2+2e^-$ transfer mechanism is also plausible where the partial reduction of oxygen ($2e^-$) can occur, desorbing the intermediate (release) and then the reaction product is further reduced ($2e^-$) on the same site or an adjacent active site[7].

ORR processes follow different ET mechanisms and pathways depending on the electrolyte media (acid and alkaline) and on the type of electrocatalyst[8,9]. For inorganic electrocatalysts, the identification and enumeration of the active sites on the surface, the morphological features such as porosity and surface area, the reaction(s) occurring on these electrocatalysts and their limiting kinetics steps are of utmost importance for understanding the ET mechanism and to potentially improve the electrocatalytic activity during ORR. With biological electrocatalysts, ORR-related charge transfer process is being integrated in several hierarchies of scale in molecular, intracellular and exocellular arrangements[10].

In general, a range of possibilities exist for inorganic electrocatalysts as they can follow a direct $4e^-$ transfer mechanism over platinum group metal (PGM) electrocatalysts[11] or a $2e^-$ transfer mechanism over pure (metal-free) carbonaceous-based electrocatalysts[12] and when metallic impurities or metallic oxides/carbides/nitrides are present in the carbon matrix[13,14]. On a platinum group metal-free (PGM-free) electrocatalyst, $2e^-$, $2+2e^-$ (same active site or different active site) and $4e^-$ transfer mechanism can occur on metal coordinated with nitrogen (M-N-C) active sites (Figure 1.A-E)[7]. The above description can be considered true only if the electrocatalyst operates in a clean circum-neutral electrolyte environment. In general, electrolytes used in bioelectrochemical systems contain molecules or charged species that bind directly with the active sites and deactivate them. Therefore, the active sites are poisoned and no longer active towards ORR and as consequence, the ORR is occurring over the carbon matrix. In the latter conditions, secondary catalyst properties such as high porosity and high surface area, contribute significantly to the ORR kinetics.

PLEASE ADD HERE FIGURE 1

In the case of enzymes, the ET mechanism follows a $4e^-$ transfer mechanism occurring in two $2e^-$ steps on the same active site without the desorption (release) of the intermediate. The first process is the rate limiting[15]. For living biocatalysts, the bacterial respiration of oxygen occurs through enzymes of the hemi-copper oxidoreductase superfamily that act as redox proton pumps in the membrane-respiratory chain of bacterial cells that conserve part of the free energy released by the ORR to generate a proton motive force. They are associated with small hemoproteins (cytochromes*)* which play the leading role as electron transporters. Generally, the amount of bioavailable oxygen impacts the cellular synthesis of the oxidoreductases catalysing the ORR. Multiple mechanisms are simultaneously involved when both biotic and abiotic catalysts are being present and described in the literature[4].

The reagents and the products involved in acidic and alkaline media electrolyte during ORR and their relative potentials are summarised in Supplementary Figure 1. It was shown that, for inorganic electrocatalysts, acidic mechanism occurs through the inner-sphere ET reaction with a direct ET. Instead, in alkaline environments, outer-sphere (OHP) ET reaction is expected with hydroxyl working like a mediator[8,9] (Figure 1F-H). Circum-neutral pH stands in the centre of the pH regions and understanding the ET mechanism at play under these conditions is crucial, but remains controversial and is not clearly defined. Recently, two independent studies showed that the actual transition from acidic to alkaline mechanism for Fe-N-C electrocatalyst occurs at rather alkaline pHs between 10-12 indicating that the dependence of the reaction mechanism is strongly associated with the pK_a of hydrogen peroxide deprotonation at $pK_a = 11.7$[16,17] (Figure 1.I). This observation is not necessarily true for other inorganic electrocatalysts where the mechanism shift can also occur at lower or circum-neutral pH following the mass low. It is important to underline that the local pH on the electrode surface (which could be highly basic) might differ from the circum-neutral bulk pH and thus affecting the reaction mechanisms locally[18].

Oxygen possesses unique features as it can be used without pre-treatment, is largely available in the atmosphere at no cost, space and weight, is easy to supply and it possesses a high redox potential. However, inadequate oxygen management might be deleterious to the overall biological or enzymatic reactions by being detrimental to the anaerobic/anoxic biofilm[19] and/or interfering with some anodic enzymes[20]. A well-defined physical/chemical gradient separation between anode and cathode or an oxygen scavenging system must be considered.

Oxygen is widely used as final electron acceptor in neutral media in technologies capable of delivering specific objectives such as water treatment/desalination, autonomous low-power source or sensing specific molecules such as microbial electrochemical systems (MESs) (e.g. microbial fuel cell (MFC), microbial desalination cell (MDC), microbial electrochemical snorkel, microbial electrochemical sensors)[21,22] and enzymatic electrochemical systems (EESs) (e.g. enzymatic fuel cell (EFC) or enzymatic biosensors)[23]. In these applications, the anodic reaction is coupled with the ORR in order to operate without an external power source. Typical open circuit voltages (OCVs) and cathode open circuit potentials (OCPs) with their activation overpotentials are reported in Supplementary Table 1. All the ET mechanisms known till date involving anodic and cathodic reactions are schematised in Supplementary Figure 2.

Inorganic electrocatalysts for ORR

Among non-biological (abiotic) electrocatalysts for ORR, the inorganic materials play a critical role. They are the most developed and widely used branch in practical electrocatalysis technology and are often available as commercial products. Such electrocatalysts are being widely used as cathode materials in BES systems. Inorganic electrocatalyst categories are very vast and diverse and are summarised in Figure 2.A[24].

This category can be divided in groups considering the presence/absence of platinum group metal within the electrocatalyst. It is important to point out that the role of catalyst poisons/inhibitors in circum-neutral media is ill understood, because of their natural abundance and more pronounced, because of the lower overall activity of the electrocatalysts.[3]

PLEASE ADD HERE FIGURE 2

Platinum group metal electrocatalysts. PGM materials are by far the most popular inorganic (abiotic) electrocatalysts in electrochemical technology. PGM electrocatalysts singularly or alloyed, supported on a carbon matrix (Figure 2.A), exhibit high electrocatalytic activity towards ORR in extreme pHs[9]. The initial large employment of PGM electrocatalysts in BES operating in circum-neutral conditions can therefore be considered as components inherited from more established chemical fuel cells. PGM electrocatalyst materials advancements and limitations are described in recent reviews[25-27]. In general, the PGM limiting step is the adsorption of oxygen on the active site. Importantly, the active sites in PGM electrocatalysts are prone to be poisoned easily and deactivated by several anions. Durability is a key issue when operating in BESs. In fact, after the deactivation of the PGM active sites, the carbon matrix itself operates as electrocatalyst[3,21]. At last, PGM electrocatalysts are rare and expensive materials and therefore not suitable for bioelectrochemical applications.

These important limitations pushed the scientists to look for diverse alternatives moving their attention towards materials possessing intrinsic characteristics and simultaneously facilitating high ORR activity, reducing the costs and being durable in harsh/polluted environments[11].

Carbonaceous-based electrocatalysts. Carbon-based materials are most often associated with BES systems as they support the premise of low cost and deployment at large scale unlimited by PGM materials availability. The PGM-free electrocatalysts category can also be divided into two subgroups in function of the presence or absence of transition metals within their structures named as metal-free carbonaceous-based or metal-based (PGM-free) electrocatalysts (Figure 2.A). Carbonaceous-based electrocatalysts can be used as ORR electrocatalysts or as carbon-matrix support to electrocatalysts. The most used carbonaceous-based electrocatalysts are reported in Figure 2.A[11,21,28,29]. Generally, carbonaceous-based materials possess important features that are useful for utilisation in MESs/EESs[28,29,30] by being electrically conductive while resilient to corrosion and able to operate in harsh/polluted environments. From an electrocatalytic point of view, carbonaceous-based electrocatalysts have low or no metal-containing active sites and their activity is much inferior compared to PGM operating in acidic or alkaline electrolyte. However, they possess secondary electrocatalyst properties such as high porosity and high

active surface area that are valuable characteristics for ORR by enhancing the interfacial surface and improving the mass transfer.

ORR on carbonaceous metal-free electrocatalysts features a $2e^-$ transfer mechanism[12] supporting the HPGR. Importantly, despite carbonaceous-based electrocatalysts being considered metal-free, this is not necessarily a correct assumption/speculation/fact. Indeed, impurities of transition metals (up to 1-2%wt)[31] were detected and mainly attributable to the starting materials. For example, carbon nanofiber (CNF), carbon nanotubes (CNT) and graphene are synthesised through precursors containing transition metals (e.g., Fe, Co, Mn) and impurities or nanoparticles are still detected at the end of the synthesis[13,14]. Transition metals presence in any form and coordination could contribute to catalyse oxygen reduction in a $4e^-$ mechanism or create active centres for favouring the disproportiortion of peroxide to water ($2e^-$ mechanism). The limiting step in carbonaceous electrocatalysts is implied to be the oxygen adsorption on the active site which in turn is not an electrochemical step[32,33].

Platinum group metal-free (PGM-free) electrocatalysts. An emerging group of nano-composite materials electrocatalysts that combine versatility of carbonaceous materials with selectivity and (to some extend) activity of the PGM ones are the PGM-free electrocatalysts**.** Termed often as PGM-free electrocatalysts, they contain transition metals of the first row and are often synthesised as atomically dispersed or single atom catalysts (SAC) for ORR showing high electrocatalytic activity towards ORR in neutral media demonstrating also high durability[11].

Four main types of PGM-free containing transition metal electrocatalysts can be identified as shown in Figure 2.A. PGM-free electrocatalysts derived by pyrolysis processes belong to the family of M-N-C (M=Mn, Fe, Co, Ni, Cu). Independently from the synthetic route, the M-N-C electrocatalyst surface is extremely diversified chemically and morphologically[34]. It is logical to assume that a multitude of active sites on the plane and the edge of the graphene-like lattice is involved during ORR[7,35,36,37,38]. The map of the edge and in plane active sites with $5.3<pH<9$ is shown in Figure 2.B-C with each active site being protonated or deprotonated in function of its pKa[17].

The active sites involved in ORR are the nitrogen-containing moieties (N-cyanide, N-imide, N-O, N-pyrrolic and N-pyridinic) and metal-containing particles, oxides, nitride and carbide and atomically dispersed metal coordinated with pyridinic nitrogen ($M-N_x$).[33,39-41]. An increasing content of nitrogen in the PGM-free electrocatalyst is beneficial for the electron transfer, enhancing the electrocatalyst´s conductivity and in turn, improving the electrocatalytic activity[42]. Generally, the majority of nitrogen functionalities are related to a larger peroxide production except N-pyridinic which is suspected to have peroxide consuming functionalities[34]. Metal-containing particles, oxides, nitrides and carbides can only perform a $2e^-$ reaction[7,34]. Usually the majority of these particles are removed from the electrocatalyst after acid/basic washing which process typically occurs

after pyrolysis. M-N_x (x=2,3,4) instead are the active sites mainly responsible for a direct 4e^- transfer mechanism[43]. M-N-C electrocatalyst is composed of diverse active sites operating differently during ORR and commonly, it can be claimed that an overall 2+2e^- transfer occurs[34] (Figure 1.A). In general, but not always, the limiting step in M-N-C electrocatalysts is actually electrochemical and is the intermediate transformation into the final product (peroxide reduction).

It was shown that the electrocatalytic activity is strictly related with the surface chemistry of PGM-free electrocatalysts and M-N_x and N-pyridinic active sites are beneficial for improving the overall ORR activity[44]. MFC power peaks of selected literature (Supplementary Table 2) in the past few years using PGM-free, carbonaceous-based and PGM electrocatalysts are reported in Figure 2.D. PGM-free electrocatalysts were characterized by the highest power output in MFCs. In neutral media, Fe-N-C electrocatalysts were shown to perform better compared to Co-N-C, Mn-N-C and Ni-N-C electrocatalysts (Figure 2.D)[45]. On the contrary to PGM, PGM-free electrocatalysts are extremely resilient to poisoning due to the low affinity between the metallic centre and the anions such as NO_3^-, Cl^-, ClO_4^- and SO_4^{2-} [46]. Poisoning seems to occur in the presence of NO_2^- and CN^- that deactivate the metal centre of the active site [46-48]. The durability of PGM-free electrocatalysts under operating conditions has been validated for over one-year demonstrating the reliability towards ORR for MESs[49].

Fundamentals and applications of enzymatic ORR electrocatalysis

ORR can be catalysed also by a large number of enzymes belonging to the family of copper proteins[50-51]. In biological oxygen chemistry, copper and iron active sites play a key role in both homogeneous and heterogeneous catalysis. Among copper proteins, multicopper oxidases (MCOs) (e.g. laccase, bilirubin oxidase (BOx), ascorbate oxidase (AO), etc.) catalyse the 4e^- ORR to water coupled to a substrate oxidation (*e.g.,* 2,2'-azino-bis(3-ethylbenzothiazoline-6-sulfonic acid (ABTS), polyphenols, *etc.*)[52].

Homogeneous electron mechanism of multicopper oxidases. Among the different types of electron transfer, the most studied and truly fascinating while being an extremely efficient ORR in circumneutral pH, is the homogeneous electron transfer mechanism. The reaction is based on a four 1e^- oxidation of substrate that is coupled with a 4e^- reductive cleavage of O–O bond in molecular oxygen[53].

As shown in Figure 3.A, the reaction mechanism accounts for three steps, which are: the reduction of the type 1 Cu^{II} site (T1Cu) site through the electrons transferred from a substrate (or electrode considering the immobilised enzyme) (step 1), the internal ET (IET) or tunnelling between the T1Cu and Trinuclear Cu Cluster (TNC) proceeding through the Cys-$(His)_2$ bridge over a distance of 13 Å (step 2) and O_2 reduction taking place at TNC[54] (step 3). The ORR mechanism is displayed in detail in Figure 3.B (homogeneous mechanism). The enzyme in its fully reduced state reacts with O_2 generating

a peroxy intermediate (PI)[55]. Next, PI is further reduced to the native intermediate (NI) through the reductive O–O bond cleavage associated with the formation of T3μ_2OH bridge[56]. NI can be rapidly reduced both through mediated ET (MET) and direct ET (DET) pathways to the initial fully reduced state, while other side reactions are really slow (oxygen atom decay with water rejection k =0.034 s^{-1}) and unlikely to occur. Therefore, the 4e^- enzymatic ORR from O_2 to H_2O occurs in two 2e^- steps. Importantly, the first step (peroxide formation) is the rate limiting, but the electron donor oxidation is considered the overall rate limiting step in the enzyme-catalysed ORR[52].

Heterogeneous electron transfer mechanism of multicopper oxidases. The heterogeneous electron transfer occurring over MCOs provides the knowledge of how DET occurs with enzymes immobilised on electrode surfaces. Once the MCOs are immobilised on air-breathing or fully immerged electrodes, the kinetics of the enzyme ET might be affected by the immobilisation method[58-59], as shown in Figure 3.C (heterogeneous mechanism).

PLEASE ADD HERE FIGURE 3.

Considering the MCOs connected in DET motion, the proper enzyme orientation and the potential applied at the electrode are mainly limiting the step 1 (the reduction of the type 1 Cu^{II} site (T1Cu) site through the electrons transferred from a substrate)[54]. The distance between the T1 and the electrode needs to be shortened as much as possible in order to ensure a fast ET. Moreover, the enzyme layer stability (e.g. enzyme leaching or structural reorganisation) might also significantly impact the step 1[60]. Different from the homogeneous mechanism, the IET (step 2) between the T1 site and the TNC might be considered as a limiting step. For example, it was demonstrated that for BOx immobilised onto graphite electrode through diazonium coupling, the rate limiting step at high pH is the IET (step 2), while at pH 5 the step 1 was prevalent[61]. The ORR occurring at TNC (step 3) is usually a fast process with apparent bimolecular constants of about 10^6 M^{-1} s^{-1}, thus it cannot be considered as a limiting step[62]. From the electrochemistry point of view, the O_2 diffusion towards the electrode surface (step 4) might also be included as a rate-limiting step. To tackle all conventional DET limiting steps, the possibility was recently proposed to pump electrons directly through the TNC (step 5) to catalyse the ORR[63]. By considering that the enzyme is immobilised according to MET configuration, three additional limiting steps have been identified. In particular, we must consider as limiting step the ET between the electrode and the redox mediator (step 6) and the ET between the redox mediator and the enzyme (step 8). When the redox mediator is a redox polymer (e.g., osmium redox polymers), we should also consider the ET within the redox mediator (step 7) as a limiting step[64].

Immobilisation methods and applications for enzymatic ORR. In order to enhance the durability and the stability of the enzymes as well as their electrochemical activity, immobilisation strategies are of critical importance for both DET and MET electrocatalysis. Despite the presence of many limiting steps, MCOs have been immobilised onto carbon-based nanomaterials by using several immobilisation methods (e.g., amide bonds formation through 1-ethyl-3-(3-dimethylaminopropyl)carbodiimide and *N*-hydroxysuccinimide (EDC-NHS) chemistry or Schiff-base intermediate, supramolecular chemistry, etc.) as shown in the Figure 3.D[65]. In addition, MCOs modified electrodes have been largely employed as enzyme-based fuel cells (EFCs)[52], amperometric biosensors[66] and pH-switchable (bio)molecule release electrodes[67], as schematically shown in Supplementary Figure 3 (A-C)[68-73]. MCOs can be successfully applied in different niche fields but there are significant barriers for their use on a large industrial scale due to high cost of the enzymes, limited durability, limited pH ranges (4-7), and low current densities because of low surface coverage.

Bacterial electrocatalysis of ORR

Biofilms of aerobic electroactive bacteria that directly or indirectly use electrodes as metabolic electron donors (biocathodes) can also act as ORR electrocatalysts. This concept has been documented since the 1980s in the field of metals biocorrosion[74] and applied in MFCs since 2005[75]. The formation of these bacterial biofilms on the electrodes is a spontaneous process towards which researchers usually lack concrete tools or technological drivers to precisely control their implementation on the electrodes.

Several parameters can potentially impact the growth and the electrocatalytic activity of the electroactive biofilm (EAB) as depicted in Figure 4.A-D[76]. The relationships that link the multi-scale properties of electrode materials and their effects on the formation, organisation and electrochemical activity of biofilms are reported in the Supplementary Figure 4. Despite the spontaneous formation of bacterial biofilms, several multidisciplinary approaches have been used to design and optimise electrode-bacterial biofilm interfaces. Moreover, electroautotrophic bacterial communities that catalyse ORR have been investigated with respect to both the rates and the mechanisms of extracellular ET (EET) between electrodes and bacterial biofilms.

PLEASE INSERT HERE FIGURE 4

EET in aerobic bacterial biofilms. Extracellular electron transfer is one of the major charge transfer mechanisms enabling the utilisation of microbial bio-cathodes in BES. In bacterial ORR cathodes, the fundamental processes ensuring the EET from the electrode material to the final electron acceptor in solution, i.e. dissolved oxygen (DO), are still quite unknown and subject to much investigation and continued discussion. Nevertheless, several direct or indirect mechanisms, more or less speculative, have been proposed by analogy with the mechanisms already described in the EAB during oxidation[77], originating

366 the concept of bidirectional EET mechanisms[78]. Analogies with the oxidation mechanisms
367 of insoluble natural electron donors as described in the iron and manganese cycles have
368 also been speculated[79]. Ultimately, ORR mechanisms highlighted in the field of marine
369 corrosion[4] have been suggested including direct ORR electrocatalysis by bacterial cells,
370 extracellular enzymes (superoxide dismutases, catalases, peroxidases) or autoxidation of
371 compounds released by microbial cells (prosthetic groups, porphyrins, haem compounds
372 and other biomolecules)[80] and also indirect ORR electrocatalysis driven by intermediates
373 produced by microbial cells[4].
374
375 **Bacterial electrocatalytic biofilms on cathode.** The electroactive biofilm forming on the
376 electrode surface is critical in practical deployment of BES and the central phenomena of
377 such systems´ operational stability and field use. Pure and complex bacteria inoculum and
378 different electrode materials were predominantly used for bacterial ORR biocathodes[4].
379 Three different methods are commonly shared for the conception of ORR bacterial
380 cathodes. The first one is based on the natural ability of aerobic biofilms to grow
381 spontaneously on material surfaces under OCP conditions[81]. The second one relies on the
382 polarisation of the electrode at a potential lower than the OCP and particularly at varied[82]
383 or controlled constant potential[83] and the third one counts on the inversion of the polarity
384 of already established bacterial anodes[84]. These reversible bacterial electrodes benefit from
385 a large biomass that develops preferentially during the cathodic phase. Periodic
386 permutation allows the neutralisation of acidification during the cathodic phase and
387 alkalisation during the anodic phase, leading to the perpetuation of the electrocatalytic
388 efficiency in the long-term[85].
389
390 **Biocathode applications.** The development of cathodic biofilm in MFCs is an emerging
391 trend in BES design and it has received much attention in the past years. Given the number,
392 versatility and co-occurrence of possible EET mechanisms that have been reported or
393 speculated, the bacterial electrocatalysis of ORR is certainly at the nexus of many different
394 pathways that could be activated or inhibited depending on the inoculum, electrode
395 materials, conditions of aerobic biofilm formation and operation, and environmental
396 parameters impacting the microbiology of the system. Different values of ORR half-wave
397 potential have been reported using voltammetric techniques[86-89]. They can be categorised
398 into two distinct groups. The first group, bacterial ORR electrocatalysis occurs at rather
399 low potentials, ranging from -0.1 to 0.1 V/SHE (System I[90]). In the second group, ORR
400 operates at higher potentials, in the range of +0.4 to +0.5 V/SHE (System II[90]). The half-
401 wave potentials of the System I or II are not correlated with the inoculum source or the
402 electrode material[90]. Due to its higher redox potential, System II is of great interest for
403 designing efficient ORR bacterial cathodes for MFC applications. The initiation of System
404 II appears to be closely related to DO bioavailability, shear rate and electrode potential
405 during the establishment of the biocathode. Most of the work reports current densities of

406 generally less than 1 A m^{-2}, except one study[91] which reveals a current density of about 3-
407 4 A m^{-2} due to an improved gas-liquid oxygen transfer.
408
409 **Limiting factors in existing bacterial ORR cathodes.** The maximum performance of
410 oxygen microbial biocathodes is not yet up to the level of the best abiotic cathodes, but
411 they offer other unrivalled advantages in terms of stability and resilience of their
412 electrocatalytic activity when exposed in complex and polluted aqueous electrolytic
413 solution (wastewater, leachate, etc.). The low availability of DO (~0.24 mM), the small
414 amount of aerobic biofilm colonising the cathode, and the multiplicity of redox microbial
415 systems catalysing the ORR are among the principal reasons explaining the poor
416 performance of oxygen microbial cathodes[4,92].
417 Several methods for optimising DO and providing extra convective oxygen transfer
418 in the aqueous electrolyte[91] by stirring, forced aeration and air pumping have proven to be
419 successful but remaining expensive alternatives. To overcome the problems, new
420 intensification paths as floating systems[94] of ORR bacterial cathodes (Supplementary
421 Figure 5.A) and passive air breathing bacterial cathodes[94] (without abiotic electrocatalyst)
422 have been recently successfully validated (Supplementary Figure 5.B). The integration of
423 planktonic microorganisms that produce DO in the electrolyte solution is also being
424 studied[95].
425
426 **Limitations by bacterial colonisation of electrode surfaces.** Bacterial biocathodes
427 encounter several limitations that are being viewed from both nature of the microorganisms
428 and their metabolism and the chemistry and morphology of the electrode, playing the role
429 of biofilm substrate. Microscopic analysis of bacterial ORR cathodes reveals
430 heterogeneous colonisation structures on the cathode[87]. Indeed, aerobic biofilms self-
431 organise in response to low DO, which is enhanced with increasing thickness of the
432 biofilms (Supplementary Figure 5.C-E). Thus, under limiting oxygen bioavailability,
433 biofilm patterns either take the form of thin layers containing only a few superimposed
434 layers of bacteria, independent, isolated adherent colonies, or networks of biofilm clusters
435 interconnected with the electrode through parts serving as electron gates[96].
436 However, increasing the amount of biofilm and the number of electroactive
437 bacterial cells on the cathode surface remains a major challenge. Electrode designs or
438 engineering systems need to maximise DO transfer leading to massive and homogeneous
439 colonisation rates. The modification of electrode surfaces[97] with increased hydrophilicity
440 allows a more homogeneous electroactive biofilm distribution. The reversible electrode
441 method leads to dense biofilm thicknesses that significantly restrict the oxygen penetration
442 to the inner layers. The bidirectional EET mechanisms seem to be less effective than those
443 occurring in conventional ORR bacterial cathodes[89].
444
445 ## Cathode architecture and upscaling

The integration of electrocatalysts into the cathode electrodes and architecture optimisation of electrodes are two key points. The integration of the electrocatalyst into the cathode architecture led to several issues related to transport phenomena and effects of chemical and physical nature ranging from angstrom/nanometric scale, up to micrometric scale, summarised in Figure 5.A where SEM images of Fe-N-C (Figure 5.B)[98], BOx cartoon representation (Figure 5.C), manganese oxides/C (Figure 5.D)[99] and single bacterium (Figure 5.E)[100] are also inserted into a spatial scale for understanding their involvement at different physical/chemical levels.

Cathode fully immerged into an aqueous solution and cathode open to air are the two main cathode configurations used in MESs or EESs[21]. The first configuration (cathode fully immerged), in order to improve the interface electrocatalyst-electrolyte, the electrode surface has to be completely hydrophilic. Importantly, the reaction occurs in a two-phase interface, liquid (protons and DO) and solid (catalytic sites). Particularly, DO is needed for bacterial ORR.

As the ORR is often limiting for MESs and EESs, a larger oxygen concentration is needed and therefore the gaseous oxygen transport is more efficient compared to the DO (~8.6 mM vs. ~0.24 mM). Instead, the second configuration (open-to-air cathode-type) operates with passive oxygen transfer based on natural diffusion phenomenon avoiding oxygen transfer through energy-consuming devices[101].

PLEASE INSERT HERE FIGURE 5

Air-breathing gas-diffusion electrode architecture. This particular cathode structure is designed particularly for enhancing the three-phase interface (TPI) as represented in Figure 7.F. In the ideal point, the TPI zone is ensured and the ORR occurs optimally. Three different phases (liquid, gaseous and solid) are involved playing a crucial role within the ORR. The liquid phase is responsible for the proton transport to the catalytic centre; the gaseous phase is responsible for the gaseous oxygen transport to the active site and the solid and conductive phase is responsible for the electron transport [21]. Therefore, the cathodes are mainly built using a pellet-type structure composed by carbonaceous-based/electrocatalyst mixture pressed over a carbonaceous or metallic porous current collector (CC)[102]. A rigorous air-breathing cathode design might optimise each single phase and merge these optimisations within the structure. Both enzymes and inorganic electrocatalysts find their optimal operation conditions once integrated in this cathode architecture. Another layer, named as diffusion layer/layers, might be added on the CC facing the air for increasing the hydrophobicity gradient and/or containing the liquid electrolyte.

Scaling up the cathodes is of paramount importance for the bioelectrochemical technology development and deployment. Images of successful pilot scale adopting large scale air-breathing cathodes are presented in Supplementary Figure 6.

Conclusions and perspective

Oxygen reduction electrocatalysis plays a central role in technical electrochemistry and is critical for energy conversion and energy storage. BESs provide utility in energy harvesting from ubiquitous sources (waste, environmentally available oxidizable compounds), in wastewater treatment (and particularly in high-carbohydrates containing wastewater) and in low energy-demand desalination, in environmental remediation and sites decontamination and biosensing. Designing of electrocatalysts and electrodes for ORR in BESs is being recognized as equally-important technological thrust, at par with the more invested biotic component of the BESs deserving special attention because of the fact that it could be the rate liming process. All these processes benefit by or directly utilise ORR in circum-neutral media. Complex electrocatalysis and hierarchy of scale and co-presence of living systems and inorganic interfaces at realistic technology scale is both a challenge and an opportunity. The realisation of large-scale and commercially available BESs for any of the above-mentioned applications requires focusing on key problems related to cost, durability, power density, biosensing/detection/degradation, etc. ORR is often being considered the limiting reaction in METs and EESs, therefore a substantial improvement and the right compromise among the issues discussed is to be established. The advantages and disadvantages of inorganic, enzymatic and bacterial electrocatalysts are presented in Figure 6. Similar comparison was previously presented more than ten years ago[103], however important efforts have been carried out in improving the activity and stability of PGM-free electrocatalysts and more long-term studies have been conducted highlighting previously unknown durability issues. Moreover, we have introduced also carbonaceous-based electrocatalysts, not considered up to now.

PLEASE INSERT HERE FIGURE 6

Inorganic electrocatalysts are the most technologically mature ORR electrocatalysts and are successfully deployed in both acidic and alkaline media, dominantly as PGM cathode electrocatalysts. PGM electrocatalysts meet most activity requirements of acid and alkaline fuel cell technology and are on trajectory to attain to the continuously increasing durability demands. PGM electrocatalysts are not suitable for bioelectrochemical systems because are expensive and their durability is compromise rapidly with the presence of pollutants. Recent introduction of PGM-free electrocatalysts for the mainstream chemical fuel cell provoked renewed interest in studying the ET mechanisms. These are currently studied to chart new paths for both activity and durability improvements. Major effort in shifting towards PGM-free materials is warranted to ensure broad introduction to BESs.

Carbonaceous materials are currently largely used as electrocatalysts in BESs because they offer the right compromise of cost, activity and durability. PGM-free

electrocatalysts are gaining more foothold as the demand for activity and selectivity raises. PGM electrocatalysts are still used for research purposes but due to their high cost are not suitable for practical applications. So far, the higher electrocatalytic activity is provided by M-N-C electrocatalysts showing stability and durability. Further enhancement of both activity and durability requires additional effort. An increase of the atomically dispersed M-N_x active sites should be accompanied with an increase of the accessibility to the active sites tuning the morphology. Novel synthetic routes are being examined coupled with theoretical studies and microscopic/spectroscopic tools, which all help to understand and predict the electrochemical output. Crucially, the cost of PGM-free electrocatalysts should be reduced substantially to be comparable to carbonaceous materials.

Enzymatic electrocatalysts for ORR have been deeply studied over the last decades with particular attention on the elucidation of the ET mechanism occurring in multicopper oxidases. The latter plays a key role for developing a new generation of enzymatic fuel cells overcoming the present limitations. In general, the ORR at MCOs modified electrodes is characterised by a high thermodynamic parameter with open circuit voltage being close to the theoretical value. This is associated with the high selectivity of the enzymatic electrocatalysis and the low tendency for side-reactions thus no mixed potential generation. Moreover, MCOs modified electrode exhibited relatively short lifetime. Most of the future research in enzymatic electrocatalysts for ORR would need to focus on improving the interfacial ET between MCOs and the electrode surface, and storage/operational stability, since they are suitable only for short-term applications (e.g., disposable biosensors). Some of the main future research directions will focus on electrode bioengineering and immobilisation techniques. For example, to overcome interfacial ET issues, scientists are currently involved in the electrode bioengineering in order to enhance the ET rates. The electrode bioengineering would be optimised with diazonium coupling or oxidation of amines and physical adsorption or site-directed enzyme immobilisation by the combination of site-directed mutagenesis, electro-grafting, and solid-phase synthesis methodology.

The progression of fundamental knowledge about ET mechanisms for bacterial ORR requires isolates of model aerobic bacteria catalysing ORR. Aerobic cathodic bacteria isolates are still rare[89] and their electroactivity remains quite unpredictable and difficult to manipulate[104]. However, their studies in electroanalytical BES individually, associated in co-cultures, or in the form of synthetic biofilms, would provide essential information firstly on the ET mechanisms, their induction and their effectors; but also on the cooperation phenomena and cell-cathode and cell-cell interactions existing within the more complex mixed biofilm systems.

To overcome the low solubility of oxygen in aqueous media, new engineering innovations need to be envisioned and pursued. Finally, the increase in oxygen bioavailability should naturally induce a much higher rate of bacterial colonisation of the electrodes. In the upcoming years, encapsulating bacteria onto the surface in polymer or

565 silica matrix could be used for pre-colonisation and electrode microbial colony
566 standardisation and it could be envisioned as major technology shift in microbial BESs[105].
567 The cathode architecture plays a key role to advance the BES technology. The ORR
568 electrocatalytic activity of an electrocatalyst using rotating ring disk electrode technique
569 doesn't always translate into high cathode performance once integrated into the cathode
570 structure. This observation propagates throughout every fuel cell technology including
571 BESs. Oxygen is supplied directly from ambient air via a passive delivery system,
572 preferably through an air-breathing gas diffusion electrode (GDE). This places emphasis
573 on optimised cathode architecture with designed three phase interface (TPI) to address all
574 these requirements for BES practical applications[101]. Particular attention has to be devoted
575 to the materials used as current collector and conductive matrix/electrocatalyst to find the
576 optimum cost, performance and durability. The cathode architecture has to contain
577 hydrophilic/hydrophobic features for an optimised TPI. Scaling up and industrial type
578 manufacturing of air-breathing GDEs have been implemented in BESs[106-107]. Fabrication
579 of gas-diffusion cathode with large geometrical area is limited by the difficulty of
580 homogeneous pressing/stamping with size increase. This either limits the design to
581 multiple medium-sized cathodes or calls for a different roll-to-roll fabrication technique.
582 Decrease in cost in any preparation step and consumables is also desired.
583 As the technology of bio-catalysed cathodes matures and becomes integrated into
584 practical devices, more and more engineering and design issues are being brought in to be
585 addressed, all contributing to the success of ORR kinetics in circum-neutral media.
586
587 **References**
588

589 1. Kinoshita, K. *Electrochemical oxygen technology*. vol. 30 (John Wiley & Sons, 1992).
590 2. Bard, A. J. & Faulkner, L. R. Fundamentals and applications. *Electrochem. Methods* **2**, 580–632
591 (2001).
592 3. Santoro, C., Serov, A., Artyushkova, K. & Atanassov, P. Platinum Group Metal-free Oxygen
593 Reduction Electrocatalysts Employed in Neutral Electrolytes for Bio-electrochemical Reactors
594 Applications. *Curr. Opin. Electrochem.* **23**, 106-113 (2020).
595 4. Erable, B., Féron, D. & Bergel, A. Microbial catalysis of the oxygen reduction reaction for microbial
596 fuel cells: a review. *ChemSusChem* **5**, 975–987 (2012).
597 5. Mano, N. & de Poulpiquet, A. O_2 reduction in enzymatic biofuel cells. *Chem. Rev.* **118**, 2392–2468
598 (2017).
599 6. Chen et al. Fundamentals, Applications, and Future Directions of Bioelectrocatalysis. *Chem Rev.* 120,
600 12903-12993 (2020)
601 7. Asset, T. & Atanassov, P. Iron-Nitrogen-Carbon Catalysts for Proton Exchange Membrane Fuel Cells.
602 *Joule* **4**, 33–44 (2020).
603 8. Ramaswamy, N. & Mukerjee, S. Alkaline Anion-Exchange Membrane Fuel Cells: Challenges in
604 Electrocatalysis and Interfacial Charge Transfer. *Chem. Rev.* **119**, 11945–11979 (2019).
605 9. Ramaswamy, N. & Mukerjee, S. Fundamental mechanistic understanding of electrocatalysis of oxygen
606 reduction on Pt and non-Pt surfaces: acid versus alkaline media. *Adv. Phys. Chem.* **2012**, 491604
607 (2012). **Understanding electron transfer mechanism in acid and alkaline environment**

10. Liu, Y. & Atanassov, P. Charge transfer at biotic/abiotic interfaces in biological electrocatalysis. Curr. Opin. Electrochem. **19**, 175-183 (2020)
11. Yuan, H., Hou, Y., Abu-Reesh, I. M., Chen, J. & He, Z. Oxygen reduction reaction catalysts used in microbial fuel cells for energy-efficient wastewater treatment: a review. *Mater. Horiz.* **3**, 382–401 (2016).
12. Watson, V. J., Nieto Delgado, C. & Logan, B. E. Influence of chemical and physical properties of activated carbon powders on oxygen reduction and microbial fuel cell performance. *Environ. Sci. Technol.* **47**, 6704–6710 (2013).
13. Martinez, U. *et al.* Critical role of intercalated water for electrocatalytically active nitrogen-doped graphitic systems. *Sci. Adv.* **2**, e1501178 (2016).
14. Costa de Oliveira, M. A., D'Epifanio, A., Ohnuki, H. & Mecheri, B. Platinum Group Metal-Free Catalysts for Oxygen Reduction Reaction: Applications in Microbial Fuel Cells. *Catalysts* **10**, 475 (2020).
15. Solomon, E. I. & Stahl, S. S. Introduction: Oxygen reduction and activation in catalysis. *Chem. Rev.* **118**, 2299-2301 (2018).
16. Malko, D., Kucernak, A. & Lopes, T. In situ electrochemical quantification of active sites in Fe–N/C non-precious metal catalysts. *Nat. Commun.* **7**, 1–7 (2016).
17. Rojas-Carbonell, S. *et al.* Effect of pH on the activity of platinum group metal-free catalysts in oxygen reduction reaction. *ACS Catal.* **8**, 3041–3053 (2018). **Identification of the mechanism switch in Fe-N-C electrocatalysts**
18. Popat, S. C., Ki, D., Rittmann, B. E. & Torres, C. I. Importance of OH^- transport from cathodes in microbial fuel cells. *ChemSusChem* **5**, 1071–1079 (2012).
19. Yang, J., Cheng, S., Li, P., Huang, H. & Cen, K. Sensitivity to oxygen in microbial electrochemical systems biofilms. *iScience* **13**, 163–172 (2019).
20. Chen, H., Dong, F. & Minteer, S. D. The progress and outlook of bioelectrocatalysis for the production of chemicals, fuels and materials. *Nat. Catal.* **3**, 225-244 (2020).
21. Santoro, C., Arbizzani, C., Erable, B. & Ieropoulos, I. Microbial fuel cells: from fundamentals to applications. A review. *J. Power Sources* **356**, 225–244 (2017).
22. O Simoska, O., et al. Recent Trends and Advances in Microbial Electrochemical Sensing Technologies: An Overview. Curr. Opin. Electrochem. **30**, 100762 (2021)
23. Ruff, A., Conzuelo, F. & Schuhmann, W. Bioelectrocatalysis as the basis for the design of enzyme-based biofuel cells and semi-artificial biophotoelectrodes. *Nat. Catal.* **3**, 214-224 (2020).
24. Wang, X. X., Swihart, M. T. & Wu, G. Achievements, challenges and perspectives on cathode catalysts in proton exchange membrane fuel cells for transportation. *Nat. Catal.* **2**, 578–589 (2019).
25. Meier, J. C. et al. Design criteria for stable Pt/C fuel cell catalysts. *Beilstein J. Nanotechnol.* **5**, 44–67 (2014)
26. Yao Nie, Y., Li, L., & Wei, Z., Recent advancements in Pt and Pt-free catalysts for oxygen reduction reaction. *Chem. Soc. Rev.* **44**, 2168-2201 (2015)
27. Gasteiger, H.A., Kocha, S.S., Sompalli, B., Wagner, F.T. Activity benchmarks and requirements for Pt, Pt-alloy, and non-Pt oxygen reduction catalysts for PEMFCs. *Appl. Catal. B: Environ.* **56**, 9–35 (2005)
28. Sharma, M. *et al.* Electrode material properties for designing effective microbial electrosynthesis systems. *J. Mater. Chem. A* **7**, 24420–24436 (2019).
29. Wang, Z., Cao, C., Zheng, Y., Chen, S. & Zhao, F. Abiotic oxygen reduction reaction catalysts used in microbial fuel cells. *ChemElectroChem* **1**, 1813–1821 (2014).
30. Minteer, S., Atanassov, P., Luckarift, H. & Johnson G. New materials for biological fuel cells. *Materials Today* **15**, 166-173 (2012)
31. Kodali, M., Santoro, C., Herrera, S., Serov, A. & Atanassov, P. Bimetallic platinum group metal-free catalysts for high power generating microbial fuel cells. *J. Power Sources* **366**, 18–26 (2017).

32. Y. Zhou, G. Chen, J. Zhang. A review of advanced metal-free carbon catalysts for oxygen reduction reactions towards the selective generation of hydrogen peroxide. *J. Mater. Chem. A* **8** (2020) 20849-20869
33. H.-T. Lien *et al*.. Probing the active site in single-atom oxygen reduction catalysts via operando X-ray and electrochemical spectroscopy. *Nat. Commun.* **11**, 4233 (2020)
34. Artyushkova, K., Serov, A., Rojas-Carbonell, S. & Atanassov, P. Chemistry of multitudinous active sites for oxygen reduction reaction in transition metal–nitrogen–carbon electrocatalysts. *J. Phys. Chem. C* **119**, 25917–25928 (2015).
35. Zitolo, A., *et al.* Identification of catalytic sites for oxygen reduction in iron-and nitrogen-doped graphene materials. *Nat. Mater.* **14**, 937-942 (2015) **Identification of the active sites in Fe-N-C electrocatalysts**
36. Zitolo, A. *et al.* Identification of catalytic sites in cobalt-nitrogen-carbon materials for the oxygen reduction reaction. *Nat. Commun.* **8**, 957 (2017)
37. Tylus, U. *et al.* Elucidating oxygen reduction active sites in pyrolyzed metal–nitrogen coordinated non-precious-metal electrocatalyst systems. *J. Phys. Chem. C* **118**, 8999-9008 (2014)
38. Jia, Q. *et al.* Spectroscopic insights into the nature of active sites in iron–nitrogen–carbon electrocatalysts for oxygen reduction in acid. *Nano Energy* **29**, 65-82 (2016)
39. Kodali, M. *et al.* High performance platinum group metal-free cathode catalysts for microbial fuel cell (MFC). *J. Electrochem. Soc.* **164**, H3041-H3046 (2017)
40. Santoro, C. *et al.* Influence of platinum group metal-free catalyst synthesis on microbial fuel cell performance. *J. Power Sources* **375**, 11-20 (2018)
41. Kodali *et al.* Enhancement of microbial fuel cell performance by introducing a nano-composite cathode catalyst. Electrochim. Acta **265**, 56-64 (2018).
42. Strelko, V.V., Kuts, V.S. & Thrower, P.A. On the Mechanism of Possible Influence of Heteroatoms of Nitrogen, Boron and Phosphorus in a Carbon Matrix on the Catalytic Activity of Carbons in Electron Transfer Reactions. *Carbon* **38**, 1499– 1503 (2000)
43. Martinez, U. *et al.* Fe–N–C Catalysts: Progress in the Development of Fe-Based PGM-Free Electrocatalysts for the Oxygen Reduction Reaction. *Adv. Mater.* **31**, 1970224 (2019).
44. Santoro, C. *et al.* A family of Fe-NC oxygen reduction electrocatalysts for microbial fuel cell (MFC) application: relationships between surface chemistry and performances. *Appl. Catal. B Environ.* **205**, 24–33 (2017).
45. Rojas-Carbonell, S., Santoro, C., Serov, A. & Atanassov, P. Transition metal-nitrogen-carbon catalysts for oxygen reduction reaction in neutral electrolyte. *Electrochem. Commun.* **75**, 38–42 (2017).
46. Ficca, V. *et al.* Effect of active sites poisoning on Fe-N-C ORR platinum group metal-free catalysts operating in neutral media: a rotating disk electrode study. *ChemElectroChem* **7**, 3044-3055 (2020)
47. Malko, D., Kucernak, A. & Lopes, T. Performance of Fe–N/C oxygen reduction electrocatalysts toward NO_2^-, NO, and NH_2OH electroreduction: from fundamental insights into the active center to a new method for environmental nitrite destruction. *J. Am. Chem. Soc.* **138**, 16056–16068 (2016).
48. Chung, M.W., Chon, G., Kim, H., Jaouen, F. & Choi, C.H. Electrochemical Evidence for Two Sub-families of FeN_xC_y Moieties with Concentration-dependent Cyanide Poisoning. *ChemElectroChem* **5**, 1880-1885 (2018)
49. Zhang, X. *et al.* Long-term performance of chemically and physically modified activated carbons in air cathodes of microbial fuel cells. *ChemElectroChem* **1**, 1859–1866 (2014).
50. Solomon, E. I., Sundaram, U. M. & Machonkin, T. E. Multicopper oxidases and oxygenases. *Chem. Rev.* **96**, 2563–2606 (1996). **Review on the electron transfer mechanisms of multicopper oxidases for ORR**
51. Solomon, E. I., Augustine, A. J. & Yoon, J. O_2 reduction to H_2O by the multicopper oxidases. *Dalton Trans.* **30**, 3921–3932 (2008).

52. Shleev, S. *et al.* Direct electron transfer between copper-containing proteins and electrodes. *Biosens. Bioelectron.* **20**, 2517–2554 (2005).
53. Calabrese Barton, S., Gallaway, J. & Atanassov, P. Enzymatic biofuel cells for implantable and microscale devices. *Chem. Rev.* **104**, 4867–4886 (2004). **Practical applications related to enzyme-based ORR**
54. Solomon, E. I., Kjaergaard, C. H. & Heppner, D. E. Molecular properties and reaction mechanism of multicopper oxidases related to their use in biofuel cells. *Electrochem. Process. Biol. Syst.* **7**, 169-212 (2015).
55. Shin, W. *et al.* Chemical and spectroscopic definition of the peroxide-level intermediate in the multicopper oxidases: Relevance to the catalytic mechanism of dioxygen reduction to water. *J. Am. Chem. Soc.* **118**, 3202–3215 (1996).
56. Yoon, J., Mirica, L. M., Stack, T. D. P. & Solomon, E. I. Variable-temperature, variable-field magnetic circular dichroism studies of tris-hydroxy-and μ_3-oxo-bridged trinuclear Cu (II) complexes: Evaluation of proposed structures of the native intermediate of the multicopper oxidases. *J. Am. Chem. Soc.* **127**, 13680–13693 (2005).
57. Yoon, J. *et al.* The two oxidized forms of the trinuclear Cu cluster in the multicopper oxidases and mechanism for the decay of the native intermediate. *Proc. Natl. Acad. Sci.* U S A **104**, 13609–13614 (2007).
58. Stines-Chaumeil, C., Roussarie, E. & Mano, N. The nature of the rate-limiting step of blue multicopper oxidases: Homogeneous studies versus heterogeneous. *Biochim. Open* **4**, 36–40 (2017).
59. Parimi, N. S., Umasankar, Y., Atanassov, P. & Ramasamy, R. P. Kinetic and mechanistic parameters of laccase catalyzed direct electrochemical oxygen reduction reaction. *ACS Catal.* **2**, 38–44 (2012).
60. Pankratov, D., Sotres, J., Barrantes, A., Arnebrant, T. & Shleev, S. Interfacial behavior and activity of laccase and bilirubin oxidase on bare gold surfaces. *Langmuir* **30**, 2943–2951 (2014).
61. Dos Santos, L., Climent, V., Blanford, C. F. & Armstrong, F. A. Mechanistic studies of the 'blue' Cu enzyme, bilirubin oxidase, as a highly efficient electrocatalyst for the oxygen reduction reaction. *Phys. Chem. Chem. Phys.* **12**, 13962–13974 (2010).
62. Lee, S.-K. *et al.* Nature of the intermediate formed in the reduction of O_2 to H_2O at the trinuclear copper cluster active site in native laccase. *J. Am. Chem. Soc.* **124**, 6180–6193 (2002).
63. Dagys, M. *et al.* Oxygen electroreduction catalysed by laccase wired to gold nanoparticles via the trinuclear copper cluster. *Energy Environ. Sci.* **10**, 498–502 (2017).
64. Gallaway, J. W. & Barton, S. A. C. Effect of redox polymer synthesis on the performance of a mediated laccase oxygen cathode. *J. Electroanal. Chem.* **626**, 149–155 (2009).
65. Singh, P. *et al.* Organic functionalisation and characterisation of single-walled carbon nanotubes. *Chem. Soc. Rev.* **38**, 2214–2230 (2009).
66. Bollella, P. & Gorton, L. Enzyme based amperometric biosensors. *Curr. Opin. Electrochem.* **10**, 157–173 (2018).
67. Bellare, M., Kadambar, V. K., Bollella, P., Katz, E. & Melman, A. Electrochemically stimulated molecule release associated with interfacial pH changes. *Chem. Commun.* **55**, 7856–7859 (2019).
68. Bollella, P., Lee, I., Blaauw, D. & Katz, E. A Microelectronic Sensor Device Powered by a Small Implantable Biofuel Cell. *ChemPhysChem* **21**, 120–128 (2020).
69. Bollella, P. *et al.* A glucose/oxygen enzymatic fuel cell based on gold nanoparticles modified graphene screen-printed electrode. Proof-of-concept in human saliva. *Sens. Actuators B Chem.* **256**, 921–930 (2018).
70. Calitri, G. *et al.* Evaluation of different storage processes of passion fruit (Passiflora edulis Sims) using a new dual biosensor platform based on a conducting polymer. *Microchem. J.* **154**, 104573 (2020).
71. Bollella, P., Melman, A. & Katz, E. Electrochemically Generated Interfacial pH Change–Application to Signal-Triggered Molecule Release. *ChemElectroChem* **7**, 3386-2403 (2020)

72. Masi, M., Bollella, P. & Katz, E. DNA Release from a Modified Electrode Triggered by a Bioelectrocatalytic Process. *ACS Appl. Mater. Interfaces* **11**, 47625-47634 (2019).
73. Bellare, M., Kadambar, V. K., Bollella, P., Katz, E. & Melman, A. Molecular Release Associated with Interfacial pH Change Stimulated by a Small Electrical Potential Applied. *ChemElectroChem* **7**, 59–63 (2020).
74. Scotto, V., Di Cintio, R. & Marcenaro, G. The influence of marine aerobic microbial film on stainless steel corrosion behaviour. *Corros. Sci.* **25**, 185–194 (1985).
75. Bergel, A., Féron, D. & Mollica, A. Catalysis of oxygen reduction in PEM fuel cell by seawater biofilm. *Electrochem. Commun.* **7**, 900–904 (2005). **ORR electrocatalysis using seawater biofilm**
76. Guo, K., Prévoteau, A., Patil, S. A. & Rabaey, K. Engineering electrodes for microbial electrocatalysis. *Curr. Opin. Biotechnol.* **33**, 149–156 (2015). **Review of electrode features for optimal electroactive biofilm development**
77. Rosenbaum, M., Aulenta, F., Villano, M. & Angenent, L. T. Cathodes as electron donors for microbial metabolism: which extracellular electron transfer mechanisms are involved? *Bioresour. Technol.* **102**, 324–333 (2011).
78. Jiang, Y. & Zeng, R. J. Bidirectional extracellular electron transfers of electrode-biofilm: Mechanism and application. *Bioresour. Technol.* **271**, 439–448 (2019).
79. He, Z. & Angenent, L. T. Application of bacterial biocathodes in microbial fuel cells. *Electroanal. Int. J. Devoted Fundam. Pract. Asp. Electroanal.* **18**, 2009–2015 (2006).
80. Freguia, S., Tsujimura, S. & Kano, K. Electron transfer pathways in microbial oxygen biocathodes. *Electrochim. Acta* **55**, 813–818 (2010). **Electron transfer mechanisms occurring in electroactive biofilm during ORR.**
81. Xu, F., Duan, J. & Hou, B. Electron transfer process from marine biofilms to graphite electrodes in seawater. *Bioelectrochemistry* **78**, 92–95 (2010).
82. Cristiani, P. *et al.* Cathodic and anodic biofilms in single chamber microbial fuel cells. *Bioelectrochemistry* **92**, 6–13 (2013).
83. Strycharz-Glaven, S. M. *et al.* Electrochemical investigation of a microbial solar cell reveals a nonphotosynthetic biocathode catalyst. *Appl. Environ. Microbiol.* **79**, 3933–3942 (2013).
84. Blanchet, E., Pécastaings, S., Erable, B., Roques, C. & Bergel, A. Protons accumulation during anodic phase turned to advantage for oxygen reduction during cathodic phase in reversible bioelectrodes. *Bioresour. Technol.* **173**, 224–230 (2014).
85. Li, W. *et al.* Simultaneous pH self-neutralization and bioelectricity generation in a dual bioelectrode microbial fuel cell under periodic reversion of polarity. *J. Power Sources* **268**, 287–293 (2014).
86. Rimboud, M., Desmond-Le Quemener, E., Erable, B., Bouchez, T. & Bergel, A. The current provided by oxygen-reducing microbial cathodes is related to the composition of their bacterial community. *Bioelectrochemistry* **102**, 42–49 (2015).
87. Desmond-Le Quéméner, E. *et al.* Biocathodes reducing oxygen at high potential select biofilms dominated by Ectothiorhodospiraceae populations harboring a specific association of genes. *Bioresour. Technol.* **214**, 55–62 (2016).
88. Rimboud, M., Bergel, A. & Erable, B. Multiple electron transfer systems in oxygen reducing biocathodes revealed by different conditions of aeration/agitation. *Bioelectrochemistry* **110**, 46–51 (2016).
89. Erable, B. *et al.* Marine aerobic biofilm as biocathode catalyst. *Bioelectrochemistry* **78**, 51–56 (2010).
90. Rimboud, M., Barakat, M., Bergel, A. & Erable, B. Different methods used to form oxygen reducing biocathodes lead to different biomass quantities, bacterial communities, and electrochemical kinetics. *Bioelectrochemistry* **116**, 24–32 (2017).
91. Milner, E. M. & Yu, E. H. The effect of oxygen mass transfer on aerobic biocathode performance, biofilm growth and distribution in microbial fuel cells. *Fuel Cells* **18**, 4–12 (2018).

92. Huang, L., Regan, J. M. & Quan, X. Electron transfer mechanisms, new applications, and performance of biocathode microbial fuel cells. *Bioresour. Technol.* **102**, 316–323 (2011).
93. Erable, B. *et al.* Marine floating microbial fuel cell involving aerobic biofilm on stainless steel cathodes. *Bioresour. Technol.* **142**, 510–516 (2013).
94. Xia, X. *et al.* Oxygen-reducing biocathodes operating with passive oxygen transfer in microbial fuel cells. *Environ. Sci. Technol.* **47**, 2085–2091 (2013).
95. Marzorati, S., Cristiani, P., Longhi, M., Trasatti, S. P. & Traversa, E. Nanoceria acting as oxygen reservoir for biocathodes in microbial fuel cells. *Electrochim. Acta* **325**, 134954 (2019).
96. Erable, B. & Bergel, A. First air-tolerant effective stainless steel microbial anode obtained from a natural marine biofilm. *Bioresour. Technol.* **100**, 3302–3307 (2009).
97. Santoro, C. *et al.* The effects of carbon electrode surface properties on bacteria attachment and start up time of microbial fuel cells. *Carbon* **67**, 128-139 (2014)
98. Miao, Z. *et al.* Atomically Dispersed Fe-Nx/C Electrocatalyst Boosts Oxygen Catalysis via a New Metal-Organic Polymer Supramolecule Strategy. *Adv. Energy Mater.* **8**,. 1801226 (2018).
99. Farahani, F. S. *et al.* MnO_x-based electrocatalysts for enhanced oxygen reduction in microbial fuel cell air cathodes. *J. Power Sources* **390**, 45–53 (2018).
100. Sanchez, D. V. *et al.* Changes in carbon electrode morphology affect microbial fuel cell performance with *Shewanella oneidensis* MR-1. *Energies* **8**, 1817–1829 (2015).
101. Wang, Z., Mahadevan, G. D., Wu, Y. & Zhao, F. Progress of air-breathing cathode in microbial fuel cells. *J. Power Sources* **356**, 245–255 (2017).
102. Zhang, F., Cheng, S., Pant, D., Van Bogaert, G. & Logan, B. E. Power generation using an activated carbon and metal mesh cathode in a microbial fuel cell. *Electrochem. Commun.* **11**, 2177–2179 (2009).
103 F. Harnisch & U. Schro¨der. From MFC to MXC: chemical and biological cathodes and their potential for microbial bioelectrochemical systems. *Chem. Soc. Rev*. **39**, 4433–4448 (2010)
104. Debuy, S., Pecastaings, S., Bergel, A. & Erable, B. Oxygen-reducing biocathodes designed with pure cultures of microbial strains isolated from seawater biofilms. *Int. Biodeterior. Biodegrad.* **103**, 16–22 (2015).
105. Luckarift, H.R. *et al.* Standardized Microbial Fuel Cell Anodes of Silica-Immobilized *Shewanella oneidensis*, *Chem. Comm.* **46**, 6048-6050 (2010)
106. Rossi, R. *et al.* Evaluating a multi-panel air cathode through electrochemical and biotic tests. *Water Res.* **148**, 51–59 (2019).
107. Hiegemann, H. *et al.* Performance and inorganic fouling of a submergible 255 L prototype microbial fuel cell module during continuous long-term operation with real municipal wastewater under practical conditions. *Bioresour. Technol.* **294**, 122227 (2019).

Acknowledgements

Carlo Santoro would like to acknowledge the support from the Italian Ministry of Education, Universities and Research (Ministero dell'Istruzione, dell'Università e della Ricerca – MIUR) through the "Rita Levi Montalcini 2018" Fellowship (Grant number PGR18MAZLI). Support from the Italian Ministry of University and Research (MIUR) through grant "Dipartimenti di Eccellenza – 2017 – Materials for energy" (2018-NAZ-0115) is gratefully acknowledged.

Author contributions

C.S., P.B. and B.E. conducted the literature search and wrote the manuscript. P.A. and D.P. supervised the study and wrote the manuscript. All the authors have contributed to the response of the reviewers.

Competing interests

The authors declare no competing interests.

Figures

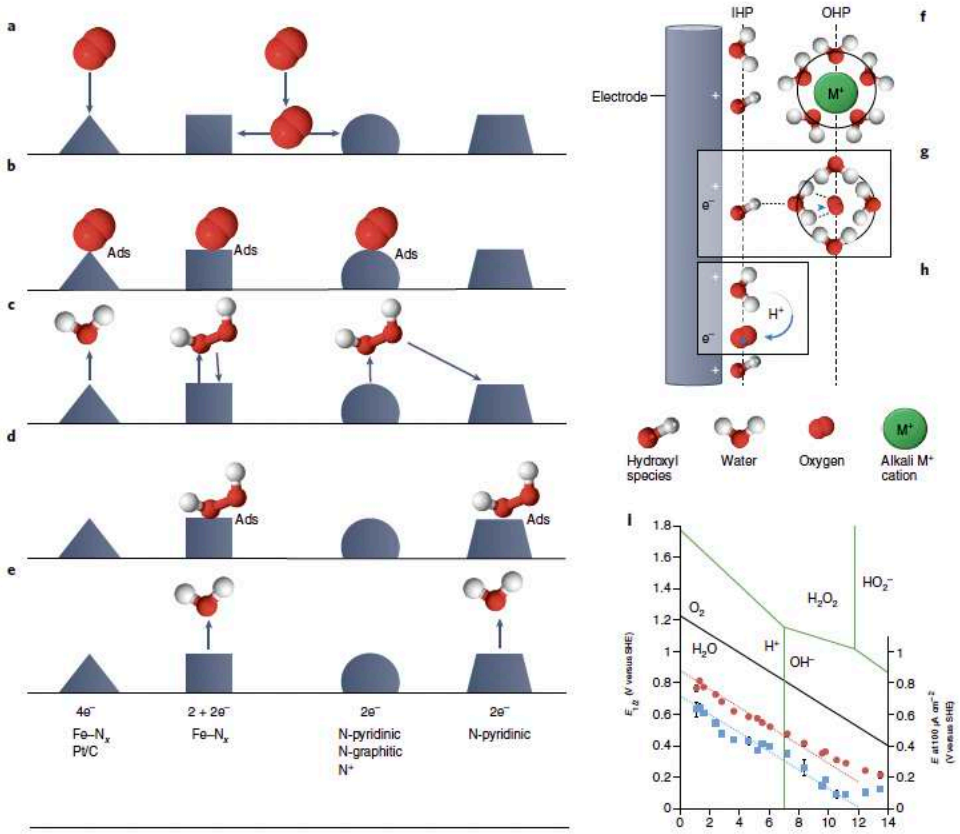

Fig. 1 Electron transfer mechanism in aqueous media for inorganic electrocatalysts

ORR mechanisms in acidic media occurring on the active sites of Fe-N-C electrocatalysts. **(a)** O_2 present in solution. **(b)** O_2 adsorption on the different active sites. **(c)** O_2 reduction into H_2O or H_2O_2 followed by the diffusion of the product in the solution. **(d)** Re-adsorption of H_2O_2 on Fe-N_x sites or N-pyridinic sites. **(e)** H_2O_2 reduction to H_2O followed by the diffusion of the product in solution. Schematic illustration of ORR in correspondence to the double-layer structure, where the inner Helmholtz plane (IHP) and the outer Helmholtz plane (OHP) are identified: **(f)** Alkali metal ions fully solvated; **(g)** O_2 fully solvated involved in outer-sphere ET processes; **(h)** O_2 partially de-solvated involved in inner-sphere ET processes. **(i)** Potential @100 μAcm^{-2} and half-wave potential ($E_{1/2}$) trends of Fe-N-C electrocatalyst measured along the entire pH projected over the Pourbaix diagram of H_2O: potential/pH diagram identifying the equilibrium phases within the aqueous electrolyte. **a-e** adapted with permission from ref.[7], Elsevier LTD. **f-h** adapted from ref.[9], Hindawi Publishing Corporation under CC BY 3.0. **i** adapted with permission from ref.[17], American Chemical Society.

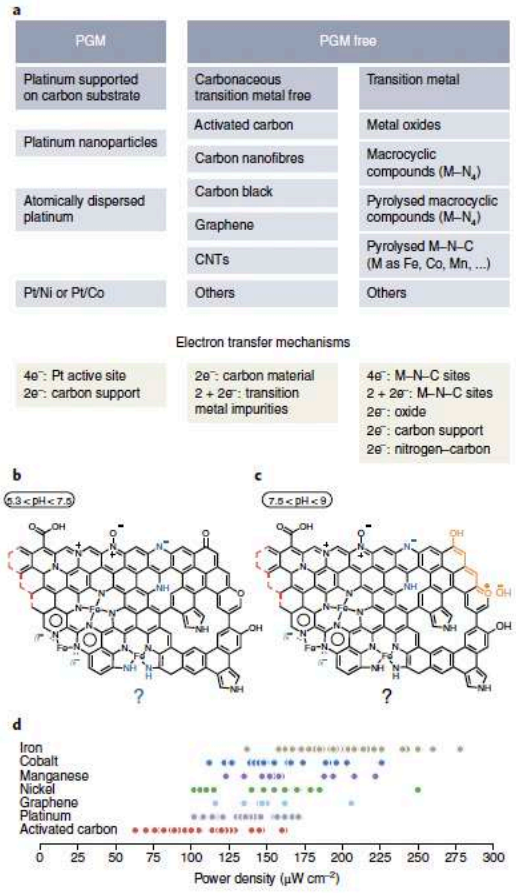

Fig. 2 Type of inorganic electrocatalysts and their electrochemical performance

(a) Categories of inorganic electrocatalysts used in BESs operating in neutral media. **(b)** and **(c)** Protonation and deprotonation of active sites in Fe-N-C electrocatalyst in working electrolyte between 5.3 and 7.5 and 7.5 and 9, respectively **(d)** Trend of power density output of MFC using different inorganic electrocatalysts. The references of the value utilised are reported in Supplementrary Table 2.
b-c adapted with permission from ref.[17], American Chemical Society.

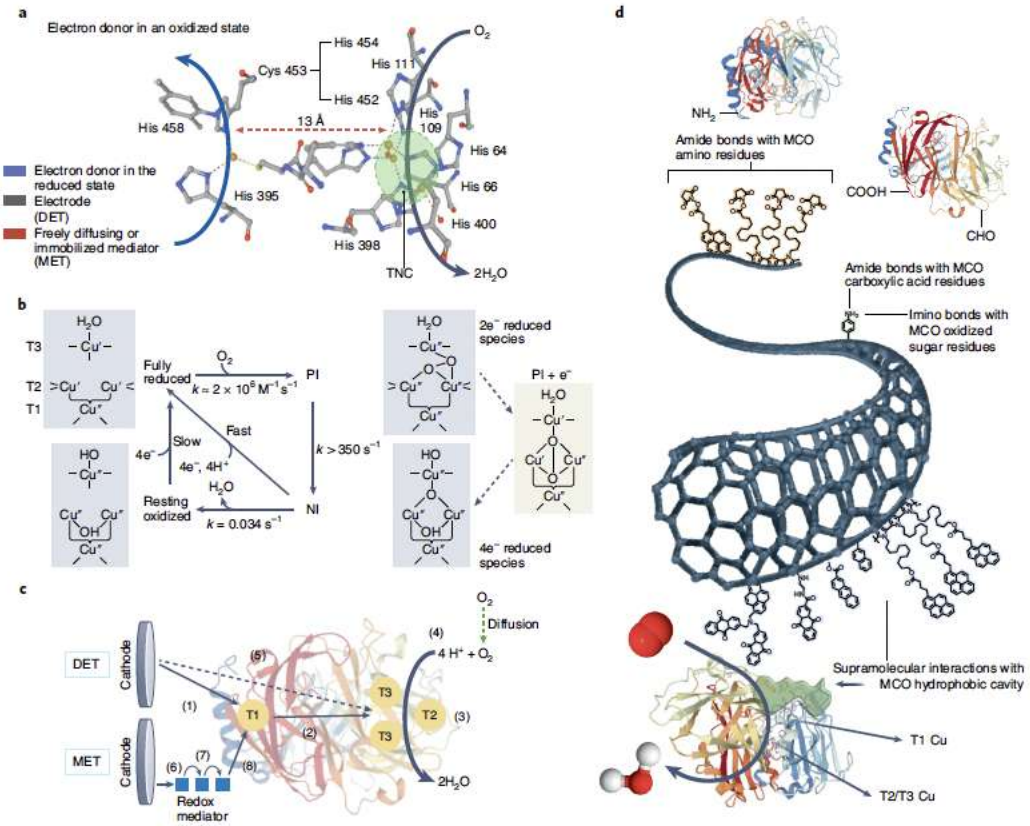

Fig.3. Electron transfer mechanism in multicopper oxidases

(a) The structure of the multicopper oxidase (MCOs) active site with arrows marking the flow of substrates, electrons (e^-) and O_2. This drawing was taken directly from the Protein Data Bank **(b)** Schematic representation of the homogeneous oxygen reduction to water occurring at the MCOs. Red arrows refer to the steps taking place in the catalytic cycle of the MCOs. Black arrows refer to the steps experimentally observed not being part of the catalytic cycle. Dashed arrows refer to the electron transfer process occurring between the PI and NI but is generally not observed in the wild type enzyme. **(c)** Heterogeneous ET mechanism of ORR occurring in direct ET (DET) and mediated ET (MET). (**d**) Different CNT functionalisation approaches for the covalent and non-covalent binding of MCOs on carbon nanotubes (CNTs) sidewalls.
a and **b** were adapted with permission from ref.[54], Wiley and Sons. **c** was adapted with permission from ref.[58], Elsevier LTD.

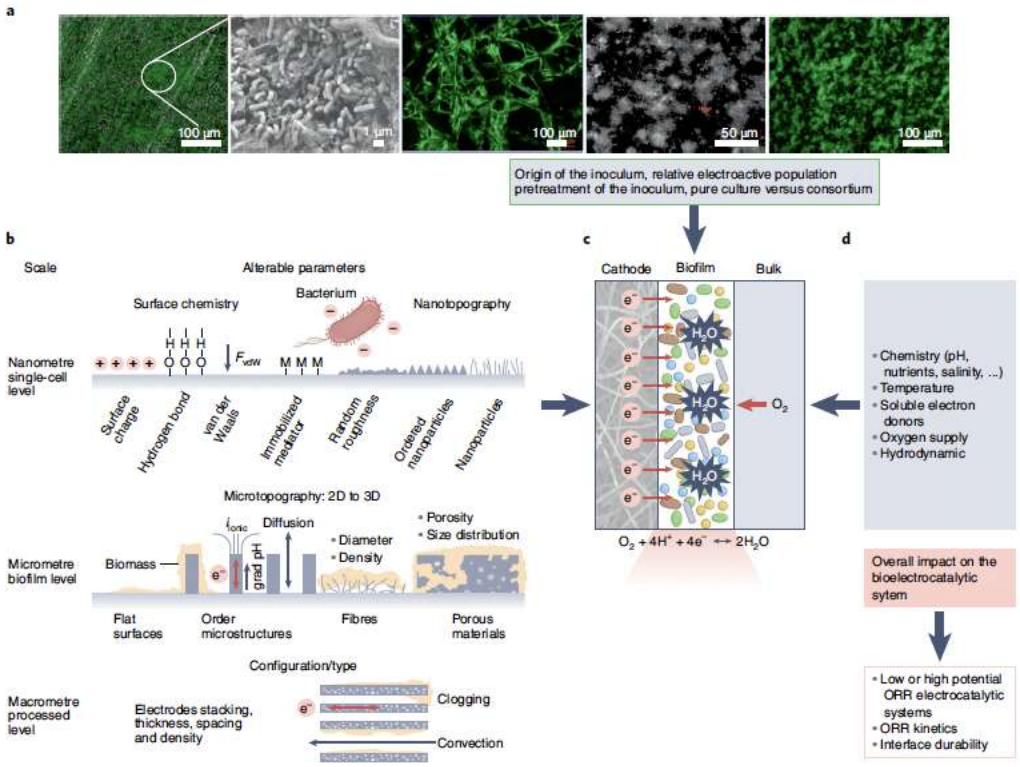

Fig. 4. Parameters affecting ORR biocathode

(a) SEM and confocal laser scanning microscopy (CLSM) images of aerobic electroactive biofilms illustrating the structural self-organisations in biofilms. **(b)** Multi-scale classification of the surface quality parameters and the structural and geometrical organisation of the electrodes. **(c)** Scheme illustrating an aerobic electroactive bacterial biofilm formed at the interface between the electrode and an aqueous electrolyte. **(d)** Physico-chemical parameters of the aqueous electrolyte solution, known to influence the development, mechanisms of EET and electrocatalytic activity of aerobic bacterial biofilms catalysing ORR. **b** is adapted with permission from ref.[76], Elsevier Ltd.

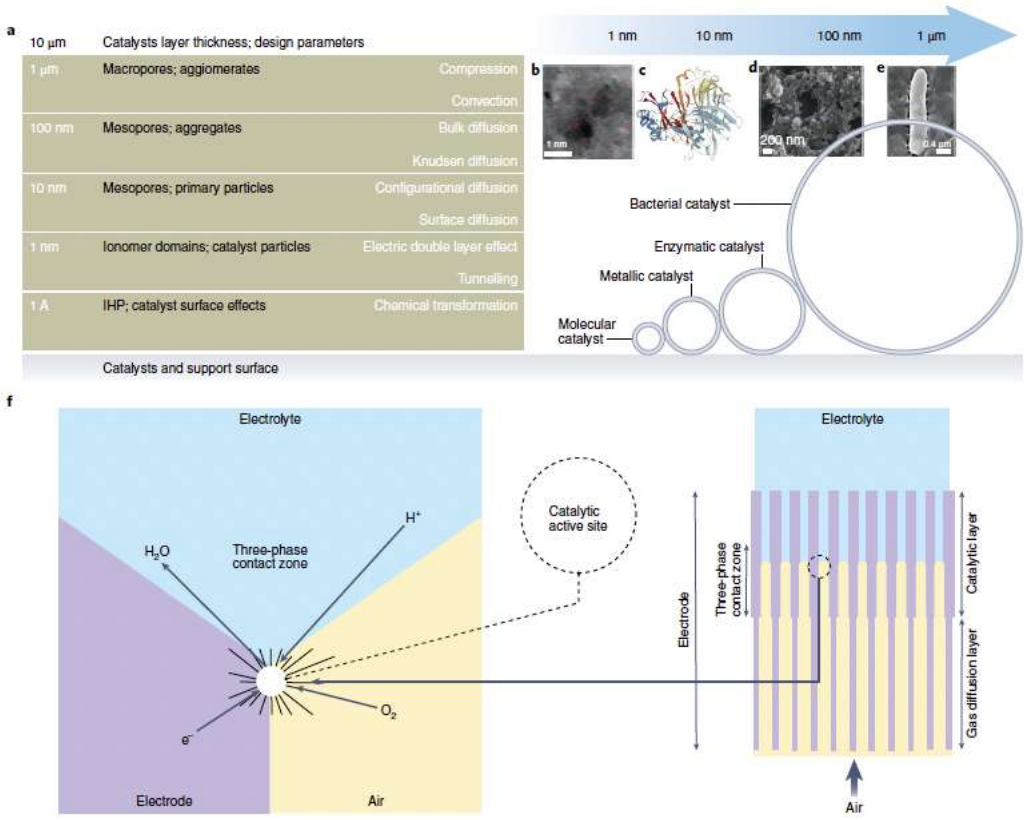

Fig. 5. Oxygen transport phenomena within the cathode architecture

(a) Transport phenomena and interaction occurring at different scale. **(b)** High-angle annular dark field scanning transmission electron microscopy of Fe-N-C electrocatalyst with subangstrom resolution. **(c)** BO_x from *Myrothecium Verrucaria*: cartoon representation of the X-ray structure. **(d)** SEM image of MnO_x/C **(e)** A magnified image of *Shewanella Oneidensis* MR-1 single bacterium. **(f)** Schematic of the three-phase interface (TPI).

b was adapted with permission from ref.[98], Wiley. **c** was adapted from Wikipedia under CC BY-SA 3.0. **d** was adapted with permission from ref.[99], Elsevier Ltd. **e** was adapted from ref.[100], MPDI under CC BY 4.0.

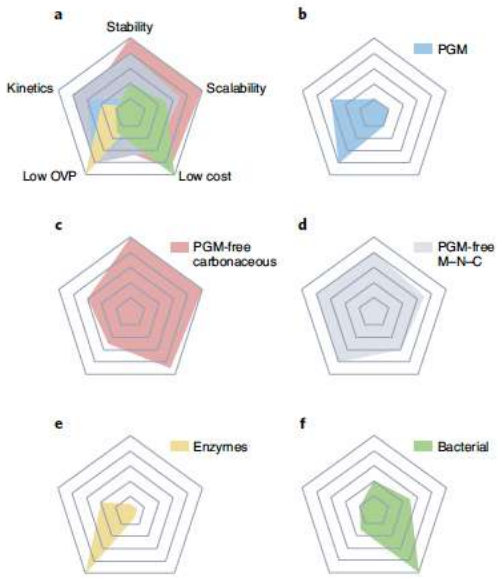

Figure 6. Key performance parameters of biotic and abiotic electrocatalysts

Overlapped comparisons of the key parameters among the different electrocatalysts used in ORR operating in neutral media (**A**). The parameters identified are stability, scalability, low cost, low OVP (overpotentials) and kinetics. Comparisons of the key parameters for single type of electrocatalysts used in neutral media ORR. **(B)** PGM, **(C)** PGM-free carbonaceous, **(D)** PGM-free metal-nitrogen-carbon (M-N-C) electrocatalysts, **(E)** enzymes and **(F)** bacteria.

Supplementary Information

Oxygen reduction reaction electrocatalysis in neutral media for bio-electrochemical systems

Carlo Santoro[1], Paolo Bollella[2], Benjamin Erable[3], Plamen Atanassov[4], Deepak Pant[5]*

[1] Department of Material Science, University of Milano-Bicocca, Building U5, Via Cozzi 55, 20125 Milan, Italy
[2] Department of Chemistry, Università degli Studi di Bari A. Moro, Via E. Orabona 4, 70125 Bari, Italy
[3] Laboratoire de Génie Chimique, Université de Toulouse, CNRS, INPT, UPS, Toulouse, France
[4] Department of Chemical & Biomolecular Engineering and National Fuel Cell Research Center, University of California Irvine, Irvine, CA 92697, USA
[5] Separation and Conversion Technology, Flemish Institute for Technological Research (VITO), Boeretang 200, Mol 2400, Belgium

Email: deepak.pant@vito.be

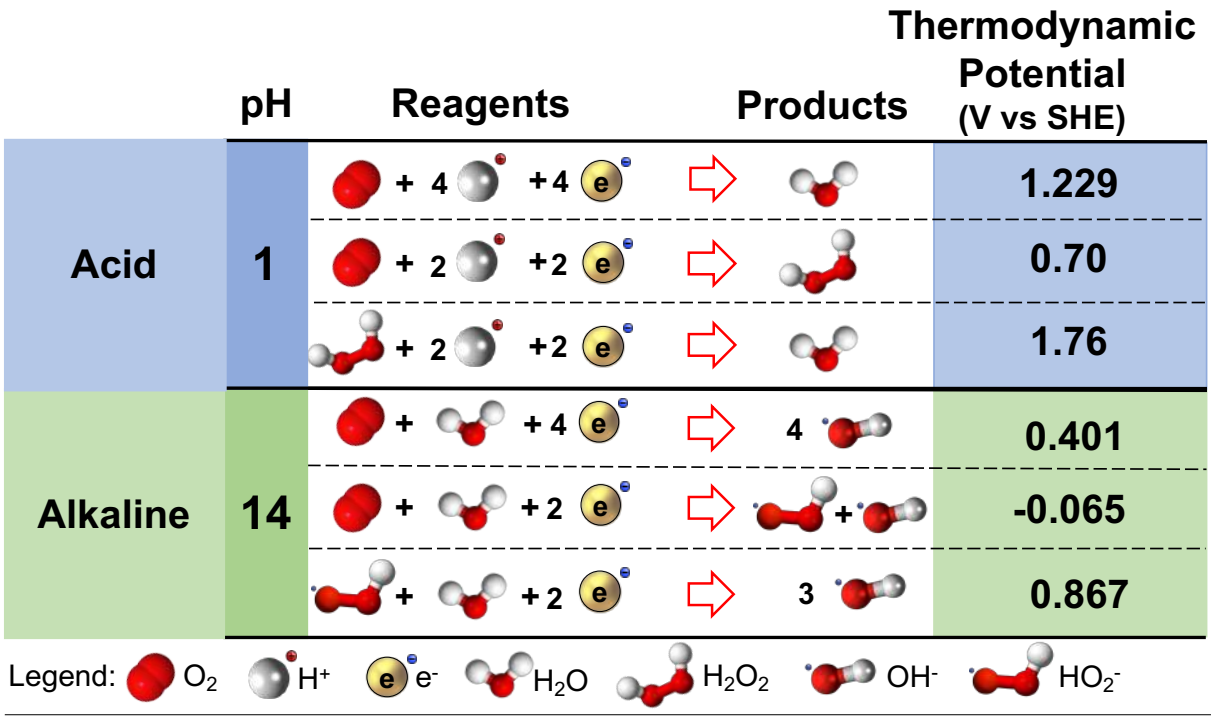

Supplementary Figure 1. ORR pathways at different electrolyte pHs and their different reduction potential at standard conditions referred versus the standard hydrogen electrode (SHE).

Supplementary Table 1. Typical open circuit voltages (OCVs) and cathode open circuit potentials (OCPs) with their activation overpotentials. Bacterial anode is speculated to operate at pH 7 using acetate as fuel with an anode potential of ≈-300 mV vs SHE.

Cathode	Cathode Potential @pH=7 mV vs SHE	Cathode Activation Overpotentials mV	OCV mV	Anode	Ref.
PGM	≈400-600	≈200-400	≈700-900	Bacterial	[1]
Carbonaceous	≈200-400	≈400-600	≈500-700	Bacterial	[1]
PGM-free	≈400-600	≈200-400	≈700-900	Bacterial	[1]
Bacterial	≈200-700	≈100-600	≈500-1000	Bacterial	[2]
Enzymatic	≈600-700	≈100-200	≈900-1000	Bacterial	[3]
Enzymatic	≈600-700	≈100-200	≈300-600	Enzymatic	[4, 5]

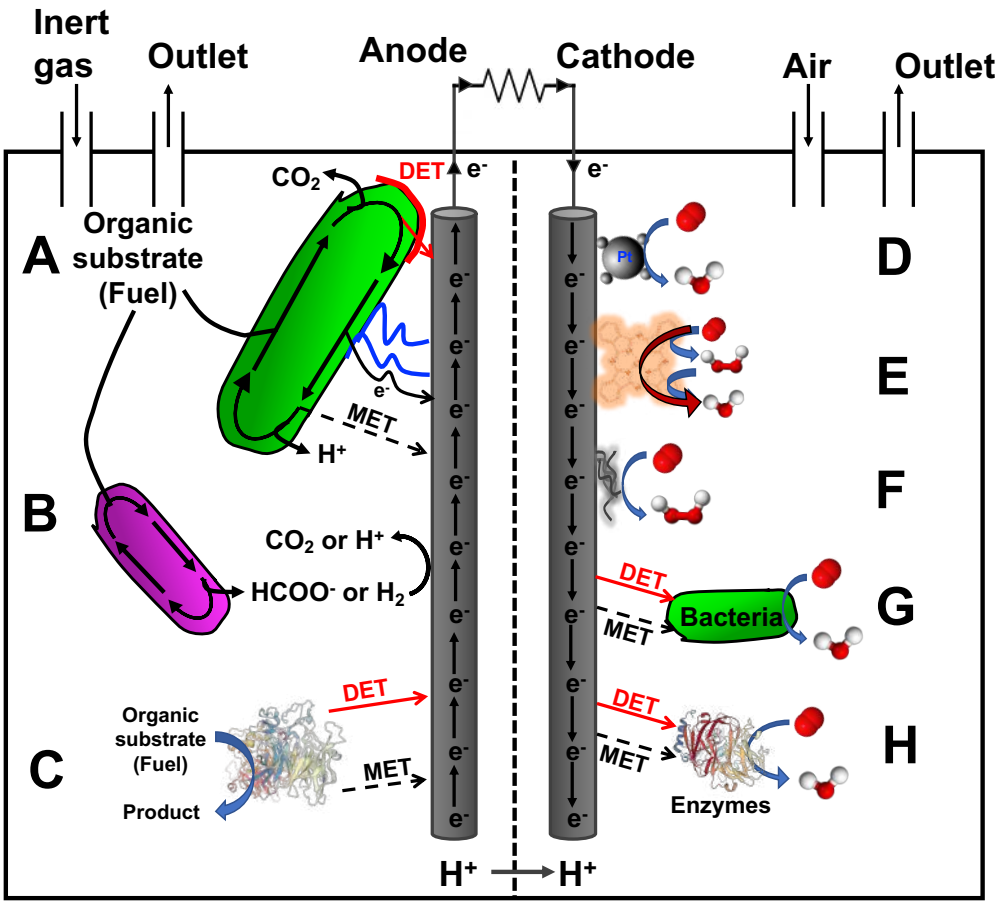

Supplementary Figure 2. (A) Oxidation reaction mechanisms occurring with bacteria through direct electron transfer, nanowires and mediated electron transfer. **(B)** Oxidation reaction mechanisms occurring with bacteria through catabolites. **(C)** Oxidation reaction occurring with enzymes via direct or mediated electron transfer. Oxygen reduction reaction schematic: **(D)** over Pt/C catalyst, **(E)** over Fe-N-C catalyst, **(F)**

over carbonaceous-based catalyst, **(G)** in presence of bacteria through direct and mediated electron transfer, **(H)** using enzymes through direct and mediated electron transfer.

Supplementary Table 2. Peaks of power curves of air-breathing cathode containing activated carbon, platinum, iron-, cobalt-, manganese-, nickel and graphene of single chamber microbial fuel cells (MFCs) are summarised in Figure 2.D in the main text. The references used for Figure 2.D are reported above.

Activated Carbon-based	mW cm^{-2}
Electrochimica Acta **2018**, 265, 56-64.	104
Journal of Power Sources **2018**, 375, 11-20.	106
Journal of Power Sources **2017**, 366, 18-26.	96
ChemSusChem **2017**, 10, 3243-3251	127
Electrochimica Acta ***2017***, 231, 115-124.	129
Applied Catalysis B: Environmental **2017,** 205, 24-33.	105
Scientific Report **2015**, 5, 16596.	117
Environmental Science & Technology **2013**, 47, 12, 6704-6710	162
Environmental Science & Technology **2013**, 47, 12, 6704-6710	63
Electrochemistry Communication **2009**, 11, 2177-2179	122
Biosensors Bioelectronics **2011**, 30, 49-55	101
Biosensors Bioelectronics **2011**, 30, 49-55	121
Environmental Science and Technology Letters **2014**, 1, 416-420	147
ACS applied materials & interfaces **2013**, 5, 7862-7866	144
RSC Advances **2012**, 2, 12751-12758	78
RSC Advances **2012**, 2, 12751-12758	91
RSC Advances **2012**, 2, 12751-12758	97
RSC Advances **2012**, 2, 12751-12758	120
RSC Advances **2012**, 2, 12751-12758	114
ChemSusChem **2016**, 9, 226-232	160
Bioresoruce Technology **2015**, 197, 318-322	140
Bioresoruce Technology **2015**, 197, 318-322	145
Bioresoruce Technology **2015**, 197, 318-322	126
Bioresoruce Technology **2014**, 163, 54-63	118
Bioresoruce Technology **2015**, 197, 318-323	70
Journal of Power Sources **2016**, 332, 447-453	123
Journal of Power Sources **2016**, 332, 447-453	120
Journal of Power Sources **2017**, 363, 87-94	92
Biosensors Bioelectronics **2019**, 127, 181-187	88
Fuel **2016**, 176, 173-180	87
Bioresource Technology **2015**, 195, 180-187	76
Journal of Electroanalytical Chemistry **2020,** 860, 113904	82
Journal of Power Sources **2020**, 450, 227683	89
Journal of Power Sources **2017**, 366, 18-26	96
Journal of Power Sources **2014**, 164, 248-253	100

Platinum-based	mW cm^{-2}
Applied Catalysis B: Environmental **2017,** 205, 24-33.	171
Energy and Environmental Science **2016**, 9, 2346-2353.	167
Scientific Report **2015**, 5, 16596.	137
Electrochemistry Communication **2009**, 11, 2177-2179	106
Environmental Science and Technology **2010**, 44, 1490-1495	161
Journal of Power Sources **2011**, 196, 1097-1102	162
ACS applied materials & interfaces **2013**, 5, 7862-7866	155
RSC Advances **2012**, 2, 12751-12758	130
Environ. Sci.: Water Res. Technol. **2017**, 3, 806-810	135
ACS Nano **2011**, 5, 12, 9611-9618	142
International Journal of Electrochemical Science **2013**, 8, 149-158	141
Scientific Report **2013**, 3, 3306	142
Science Advances **2015**, 1, e1500372	146
Journal of Power Sources **2016**, 315, 302-307	103
Biochemical Engineering Journal **2013,** 73, 49-52	139
Biochemical Engineering Journal **2013,** 73, 49-52	133
Biochemical Engineering Journal **2013,** 73, 49-52	118
Journal of Power Sources **2016**, 307, 1-11	102
Chemical Engineering Journal **2018**, 342, 395-400	136
Inorganic Chemistry Communication **2019**, 105, 69-75	108
Applied Surface Science **2020**, 505, 144547	120
Journal of Power Sources **2020**, 450, 227684	121
Electrochimica Acta **2016**, 190, 620-627	114
Journal of Power Sources **2012**, 216, 187-191	171
Journal of Power Sources **2019**, 414, 444-452	157

Graphene-based	mW cm^{-2}
Electrochimica Acta **2018**, 265, 56-64.	150
Journal of Power Sources **2017,** 356, 371-380	150
Journal of Power Sources **2017,** 356, 371-380	185
Journal of Power Sources **2017,** 356, 371-380	206
Bioelectrochemistry **2014, 95**, 23-28	116
ACS Nano **2011**, 5, 12, 9611-9618	135
Scientific Report **2013**, 3, 3306	162
Scientific Report **2013**, 3, 3306	135
Journal of Power Sources **2016**, 327, 548-556	168
Journal of Power Sources **2016**, 327, 548-556	145
Journal of Materials Chemistry A **2016**, 4, 12387-12391	147

Manganese-based	mW cm^{-2}
Electrochimica Acta ***2017***, 231, 115-124.	160
Journal of Power Sources ***2012***, 216, 187-191	150
Journal of Power Sources **2012**, 216, 187-191	208
Journal of Power Sources **2012**, 216, 187-191	147
Journal of Power Sources **2017**, 366, 18-26	222
Journal of Power Sources **2017**, 366, 18-26	188
Journal of Power Sources **2014**, 164, 248-253	135
Journal of Power Sources **2014**, 164, 248-253	155
Journal of Power Sources **2014**, 164, 248-253	123
Journal of Power Sources **2019,** 414, 444-452	194
Journal of Power Sources **2019,** 414, 444-452	158
Journal of Power Sources **2019,** 414, 444-452	152

Nickel-based	mW cm^{-2}
Electrochimica Acta ***2017***, 231, 115-124.	171
Journal of Power Sources **2016**, 327, 548-556	102
International Journal of Hydrogen Energy **2015**, 40, 1145-1153	115
Electrochimica Acta **2016**, 190, 620-627	185
Electrochimica Acta **2016**, 190, 620-627	148
Electrochimica Acta ***2016***, 219, 88-98	250
Electrochimica Acta ***2016***, 219, 88-98	155
Electrochimica Acta ***2016***, 219, 88-98	140
International Journal of Hydrogen Energy **2017**, 42, 3271-3280	169
International Journal of Hydrogen Energy **2017**, 42, 3271-3280	106
International Journal of Hydrogen Energy **2015**, 40, 5928-5938	179
International Journal of Hydrogen Energy **2015**, 40, 5928-5938	170
International Journal of Hydrogen Energy **2015**, 40, 5928-5938	140
International Journal of Hydrogen Energy **2015**, 40, 5928-5938	110
Journal of Power Sources **2017**, 366, 18-26	163
Journal of Power Sources **2017**, 366, 18-26	162

Cobalt-based	mW cm^{-2}
Journal of Power Sources **2017**, 366, 18-26.	148
Electrochimica Acta ***2017***, 231, 115-124.	196
Journal of Power Sources **2016**, 307, 1-11	112
Journal of Power Sources **2017**, 363, 87-94	191
Journal of Power Sources **2017**, 363, 87-94	164
Journal of Power Sources **2017**, 363, 87-94	127
Biosensors Bioelectronics **2019**, 127, 181-187	225
Biosensors Bioelectronics **2019**, 127, 181-187	189
Biosensors Bioelectronics **2019**, 127, 181-187	150
Biosensors Bioelectronics **2019**, 127, 181-188	139
Fuel **2016**, 176, 173-180	123
Fuel **2016**, 176, 173-180	142
Chemical Engineering Journal **2018**, 342, 395-400	154
Chemical Engineering Journal **2018**, 342, 395-400	140
Chemical Engineering Journal **2018**, 342, 395-400	122
Inorganic Chemistry Communication **2019**, 105, 69-75	126
Bioresource Technology **2015**, 195, 180-187	150
Bioresource Technology **2015**, 195, 180-187	139
Bioresource Technology **2015**, 195, 180-187	142
Chemical Engineering Journal **2020**, 385, 123861	226
Applied Surface Science **2020**, 505, 144547	174
Applied Surface Science **2020**, 505, 144547	149
Applied Surface Science **2020**, 505, 144547	145
Applied Surface Science **2020**, 505, 144547	127
Advance Energy Materials **2016,** 6, 1501498	166
Journal of Electroanalytical Chemistry **2020,** 860, 113903	203
Journal of Electroanalytical Chemistry **2020,** 860, 113904	189
Journal of Electroanalytical Chemistry **2020,** 860, 113904	155
Journal of Power Sources **2017**, 366, 18-26	148

Iron-based	mW cm^{-2}
ACS Applied Energy Materials **2018**, 1(10), 5755-5765.	162
Electrochimica Acta. **2018**. 277, 127-135.	185
Electrochimica Acta **2018**, 265, 56-64.	217
Journal of Power Sources **2018**, 378, 169-178.	180
Journal of Power Sources **2018**, 375, 11-20.	214
Journal of Power Sources **2017**, 366, 18-26.	192
ChemSusChem **2017**, 10, 3243-3251	243
ChemSusChem **2017**, 10, 3243-3251	182
Electrochimica Acta **2017**, 231, 115-124.	251
Applied Catalysis B: Environmental **2017,** 205, 24-33.	209
Applied Catalysis B: Environmental **2017,** 205, 24-33.	206
Applied Catalysis B: Environmental **2017,** 205, 24-33.	202
Applied Catalysis B: Environmental **2017,** 205, 24-33.	199
Applied Catalysis B: Environmental **2017,** 205, 24-33.	187
Applied Catalysis B: Environmental **2017,** 205, 24-33.	172
Applied Catalysis B: Environmental **2017,** 205, 24-33.	163
Journal of The Electrochemical Society **2017**, 164(3), H3041-H3046	178
Journal of The Electrochemical Society **2017**, 164(3), H3041-H3047	173
Energy and Environmental Science **2016**, 9, 2346-2353.	204
Energy and Environmental Science **2016**, 9, 2346-2353.	197
Scientific Report **2015**, 5, 16596.	167
ACS applied materials & interfaces **2013**, 5, 7862-7866	158
Journal of Power Sources **2020**, 465, 228264	250
Chemical Engineering Journal **2020**, 380, 122522	240
Bioresource technology **2017**, 233, 399-405	278
ChemSusChem **2016**, 9, 226-232	260
Journal of Power Sources **2020**, 450, 227683	226
Journal of Power Sources **2020**, 450, 227683	208
Journal of Power Sources **2020**, 450, 227684	167
Electrochimica Acta **2019**, 304, 360-369	196
Electrochimica Acta **2019**, 304, 360-369	185
Electrochimica Acta **2019**, 304, 360-369	159
Electrochimica Acta **2019**, 304, 360-369	137
Journal of Power Sources **2017**, 366, 18-26	192
Journal of Power Sources **2017**, 366, 18-26	221
Journal of Power Sources **2017**, 366, 18-26	162
Journal of Power Sources **2019**, 414, 444-452	194
Journal of Power Sources **2019**, 414, 444-452	158

986
987

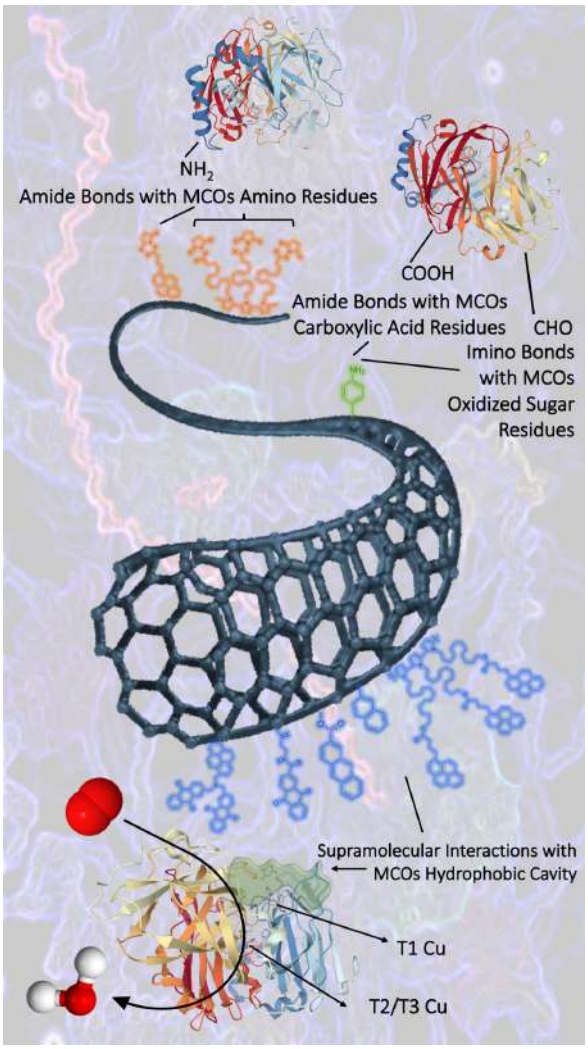

Supplementary Figure 3. Different CNT functionalisation approaches for the covalent and non-covalent binding of MCOs on carbon nanotubes (CNTs) sidewalls.

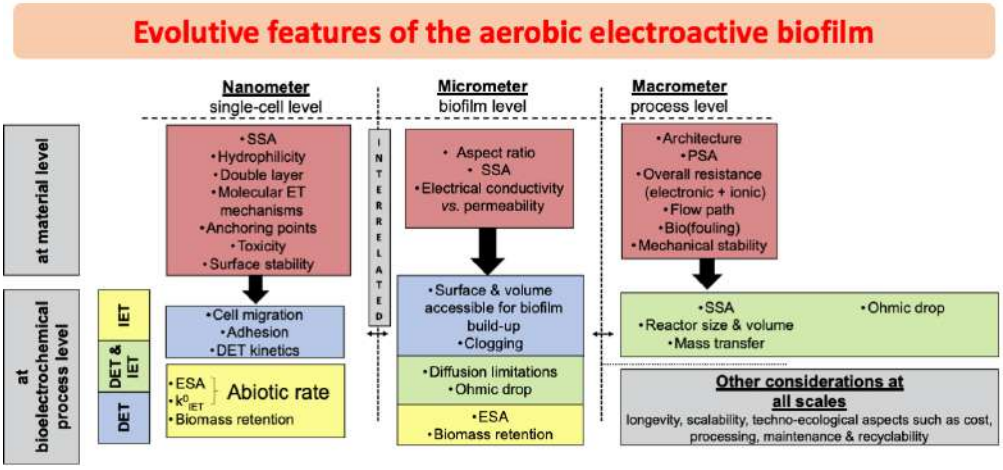

Supplementary Figure 4. Interrelationships linking the multi-scale properties of electrode materials and their consequences on the formation, organisation and electrochemical activity of biofilms. The Figure was adapted with permission from ref.[6], Elsevier Ltd.

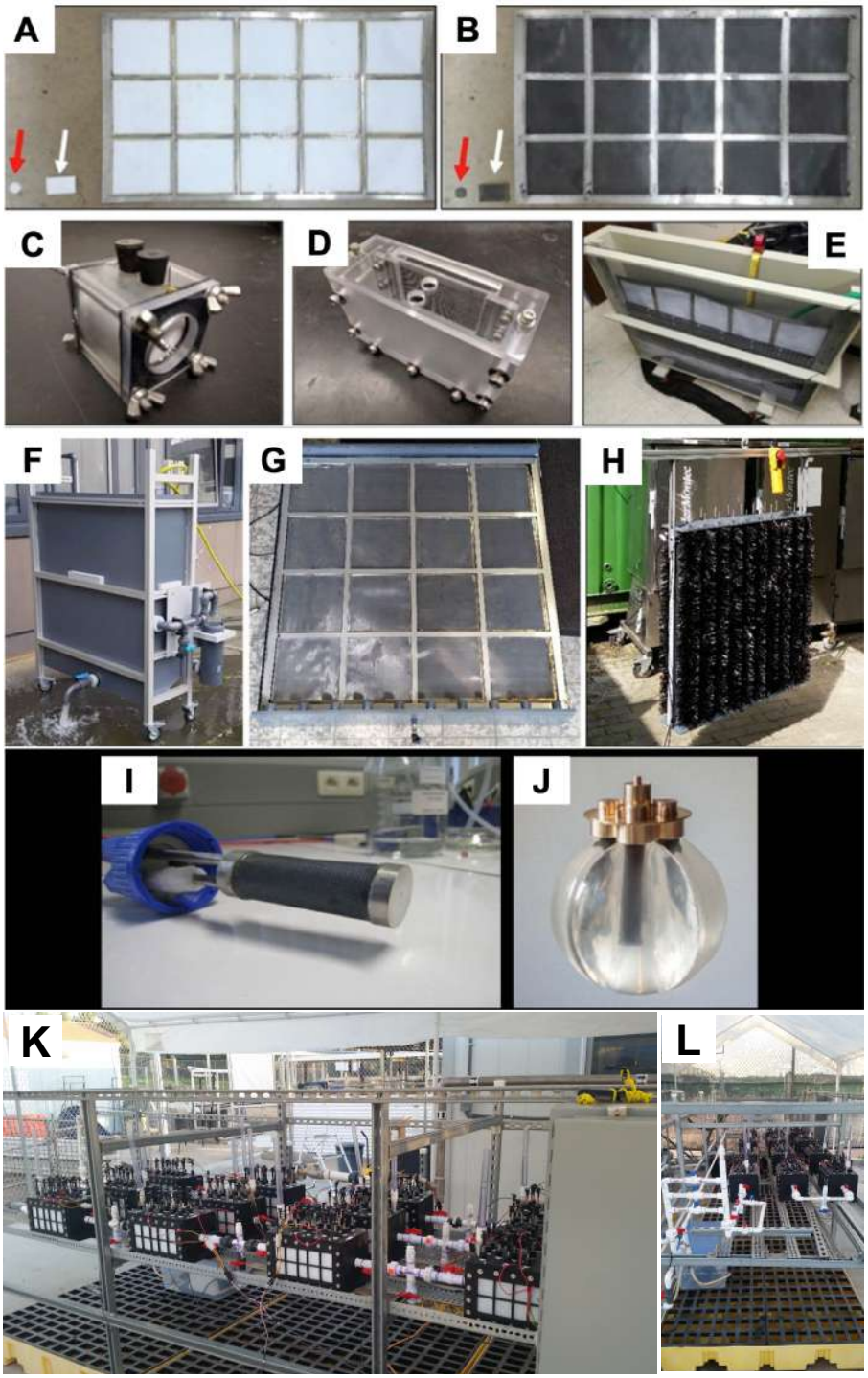

Supplementary Figure 5. GDE electrode configurations in different sizes and geometries. **(A)** Gas diffusion side of an upscaled GDE **(B)** Electrolyte exposed side of an upscaled GDE. **(C, D)** Lab scale air-cathode MFCs of 10 cm² and 100 cm². **(E)** An 85 L MFC for testing GDE shown in (A) and (B). **(F)** A 255 L MFC reactor **(G)** An upscaled GDE for testing in (F). **(H)** Graphite fibre brush anode used in (F) and tested in combination with (G). **(I)** A tubular GDE. **(J)** A 'spark of life' set up employing a GDE shown in **(I)**. Picture of the 12 MFC pilot scale while operating at the Agriculture Center at San Pasqual High School (Escondido-CA, USA). **A-E** were adapted with permission from ref. [7], Elsevier Ltd. **F-H** were adapted with permission

from ref. [8], Elsevier Ltd. **I-J** Spark of Life - Teresa van Dongen. http://www.teresavandongen.com/Spark-of-Life. **K-L** were adapted with permission from ref. [9], Wiley and Sons.

Supplementary References

1. Santoro, C., Arbizzani, C., Erable, B. & Ieropoulos, I. Microbial fuel cells: from fundamentals to applications. A review. *J. Power Sources* **356**, 225–244 (2017).
2. Erable, B., Féron, D. & Bergel, A. Microbial catalysis of the oxygen reduction reaction for microbial fuel cells: a review. *ChemSusChem* **5**, 975–987 (2012).
3. Santoro, C., Soavi, F., Serov, A., Arbizzani, C. & Atanassov, P. Self-powered supercapacitive microbial fuel cell: the ultimate way of boosting and harvesting power. *Biosens. Bioelectron.* **78**, 229-235 (2016)
4. Ruff, A., Conzuelo, F. & Schuhmann, W. Bioelectrocatalysis as the basis for the design of enzyme-based biofuel cells and semi-artificial biophotoelectrodes. *Nat. Catal.* **3**, 214-224 (2020).
5. Chen, H., *et al*. Fundamentals, Applications, and Future Directions of Bioelectrocatalysis. *Chem. Rev.* **120**, 12903–12993 (2020)
6. Guo, K., Prévoteau, A., Patil, S. A. & Rabaey, K. Engineering electrodes for microbial electrocatalysis. *Curr. Opin. Biotechnol.* **33**, 149–156 (2015).
7. Rossi, R. *et al.* Evaluating a multi-panel air cathode through electrochemical and biotic tests. *Water Res.* **148**, 51–59 (2019).
8. Hiegemann, H. *et al.* Performance and inorganic fouling of a submergible 255 L prototype microbial fuel cell module during continuous long-term operation with real municipal wastewater under practical conditions. *Bioresour. Technol.* **294**, art. No. 122227 (2019).
9. Babanova, S. et al. Continuous flow, large-scale, microbial fuel cell system for the sustained treatment of swine waste. *Water Environ. Res.* **92**, 60-72 (2020)